A STATE MODEL FOR AIRBORNE RADAR GROUND CLUTTER

By

DONALD CAROL WATSON

Bachelor of Science
Texas A and M University
College Station, Texas
1958

Master of Science
Southern Methodist University
Dallas, Texas
1963

Submitted to the Faculty of the Graduate College
of the Oklahoma State University
in partial fulfillment of the requirements
for the Degree of
DOCTOR OF PHILOSOPHY
July, 1970

A STATE MODEL FOR AIRBORNE RADAR

GROUND CLUTTER

Thesis Approved:

Bennett L. Basore
Thesis Adviser

Arthur M. Breipohl

Paul A. McCollum

Joe L. Howard

D. Durham
Dean of the Graduate College

PREFACE

This dissertation is directed at obtaining a state model of the airborne radar ground clutter stochastic process which can be applied in schemes used to discriminate against clutter. Development of the model has been based upon the change in the radar cross section of a ground resolution cell viewed from an aircraft as the aircraft changes position. The basic randomness used in the development of the process was assumed to be the random separation of reflection points within a resolution cell. The process is shown to be nonstationary.

The developed model includes the clutter process autocorrelation function which is used to obtain an approximation of decorrelation distance. The Bayesian approach to Kalman filtering is alternatively applied through use of the clutter model to obtain equations for recursive filtering.

I would like to take this opportunity to thank the chairman of my committee, Professor Bennett Basore, who is also my thesis adviser. He has always provided counseling and advice whenever they were needed. His comments and suggestions at the correct point during this study have resulted in a smooth progression of the work.

Professor A. M. Breipohl has provided unstinted assistance with the recursive filtering sections of this study. Professor P. A. McCollum and Professor J. L. Howard, the other two members of my committee, have provided sustained encouragement and thorough instruction.

The Fort Worth Division of General Dynamics has provided much

appreciated financial support.

Finally, my wife, Sammie, has contributed confidence, encouragement, understanding, and sacrifice throughout all my graduate studies.

TABLE OF CONTENTS

LIST OF FIGURES

CHAPTER I

INTRODUCTION

Airborne radar systems which view the ground are plagued with a particular type of interference phenomenon commonly called ground clutter or clutter. This clutter generally results from constructive and destructive interference between the returns from many individual scatterers, each of which is too small to be resolved by the radar. The fluctuation or variation in the return from a ground patch (cell) therefore results from relative motion between the individual scatterers with respect to the viewing radar. The dominant source of this relative motion and therefore that of clutter is usually aircraft motion rather than scatterer motion. It is the clutter resulting from aircraft motion which is considered in this thesis. This clutter will be shown to be a nonstationary stochastic process which produces a modulation of the radar cross section of a ground cell in a noise-like fashion.

Statement of the Problem

A pulsed radar may be considered a sampling device which samples the ground clutter process at some pulse repetition frequency (PRF). The degree of correlation from pulse to pulse may then be described by use of a clutter autocorrelation function, and the information obtained through use of this function is essential in most clutter discrimination schemes. Therefore, the problem considered herein is the development of

a mathematical clutter model. Solution of this problem is in part dependent on the use of the concept of radar cross section (RCS) to derive a clutter time autocorrelation function and other first-order and second-order moments of the clutter process which are necessary parts of the clutter model. The basic model developed is a discrete state model; however, it will be seen that the basic relation is the autocorrelation function.

Clutter cell radar cross section (RCS) is a random variable whose behavior characterizes the clutter process. Therefore, the clutter process is developed in terms of cell RCS. A particular cell is designated by its position on a coordinate system located at the aircraft. A single cell then is analyzed in terms of its varying RCS which is produced by changes in the aircraft viewing position with respect to the fixed position of the cell. This varying RCS is a function of aircraft motion which may be converted to a function of time through a knowledge of aircraft velocity. The statistics of the variation in cell RCS as a function of aircraft position and velocity (or time and time difference) is of primary interest because this technique can be used to develop a clutter model which will be generally applicable to most moving pulsed radars. Such a model is particularly useful since it can be related to any particular radar on the basis of a minimal number of criteria: (1) radar beamwidth and pulse width, which designate cell size, (2) wavelength, and (3) radar position and rate of change of position with respect to the reflecting surface.

The clutter model developed on the basis of the above criteria will be shown to be easily adapted to the solutions of filtering problems. It can also be used to provide insight into the clutter process.

In fact, a simple expression for decorrelation distance (or time) can be directly obtained from the autocorrelation function in terms of only antenna aperture width and antenna azimuth angle. In addition, the clutter power density spectrum at the output of a square law detector can be obtained from the Fourier transform of the clutter autocorrelation function.

Although such a model represents a nonstationary process, short-term, wide-sense stationarity will be justified and used for time-changes on the order of one radar scan time.

Approach to the Solution

This study of airborne radar ground clutter will be conducted on the basis of three major substudies. First, a state model of the clutter process will be developed. Then the state model will be analyzed by studying the resulting autocorrelation function and by studying the relationships derived from the autocorrelation function, such as process spectrum and decorrelation distance. The final substudy will be directed to developing and comparing several approaches to the application of the clutter state model.

The state model will be developed in three successive steps. A probability density function will be derived to model the basic randomness as a first step. Next, this randomness will be used in the expression of the phase of the cell-reflected voltage through the use of the geometry of aircraft motion with respect to the reflecting cell. Then a phasor addition of these voltages will be used to obtain an expression of cell radar cross section and time will be introduced by considering the cell radar cross section seen by the radar on successive pulses.

The cell radar cross section thus derived as a function of time will be shown to constitute a first-order difference equation of the state of cell radar cross section from pulse to pulse, i.e., a state model.

Analysis of the state model will be performed through a study of the developed autocorrelation function. Computer calculations of the autocorrelation function and its Fourier transform will be obtained at discrete points, and these functions will be plotted in three dimensions. Analysis of the function plots will allow the determination of several invariant properties of the clutter process. However, it will be shown that the rate of availability of clutter information is not invariant but depends upon aircraft velocity, antenna size, and antenna azimuth angle.

The final major substudy will consist of a limited study of applications. It will be limited in the sense that the clutter model will be used in a few typical applications to demonstrate its capabilities of clutter discrimination, and the application of the subject model will be compared with other clutter discrimination techniques.

Previous Work in the Area

Much of the early work done on radar clutter was accomplished at the Massachusetts Institute of Technology in the 1940's. Some of this work was documented in the Radiation Laboratory Series. Rice (1) defined a general approach which can be applied to many types of clutter power. This approach is based on the assumption that the voltage returned from individual scatterers can be divided into orthogonal components, and that the amplitude distribution of each component is gaussian and its phase distribution is uniform. When this rationale is

used, the magnitude of the square of the sum of these gaussian components results in a Rayleigh distribution for clutter power. However, this approach is often used without developing an expression for the time autocorrelation function which is the key relationship.

The airborne clutter problem has been considered under the assumption of time stationarity in several previous studies of clutter filtering (2,3,4). The sea clutter problem is closely related to the airborne clutter problem, and it has been demonstrated that sea clutter effects can be reduced through the use of a high-scan-speed radar (5). When a high scan speed is used and only one or two hits are obtained per scan, the average data rate can be kept constant while the time between successive pulses (or pulse pairs) is increased to allow time for decorrelation. Integration will then smooth the sea clutter (or ground clutter). In the similar case of airborne radars, it has also been shown that pulse-to-pulse frequency stepping (frequency agility) provides clutter decorrelation and thus facilitates clutter smoothing (6,7).

The Illinois Institute of Technology (IIT) recently used a mixture of theoretical and data studies to develop a general clutter model for predicting airborne radar performance in ground clutter environments (8). In this model, both discrete and distributed clutter are considered on the basis of generally assuming a log normal clutter distribution. The model of the triangular correlation function for distributed clutter used in the IIT study is a simplified approximation similar to the autocorrelation function subsequently developed in this thesis.

Results of a previous study done at General Electric show that one antenna aperture width is the approximate distance a radar must travel between pulses to attain pulse-to-pulse decorrelation (9). A value of

approximately one aperture width is subsequently derived in this thesis as the distance necessary for pulse-to-pulse decorrelation of clutter at an azimuth angle of 30 degrees. Completely different approaches were used in obtaining these two similar relationships.

CHAPTER II

STATISTICAL MODEL OF GROUND SCATTERER SEPARATION

The statistical model of ground scatterer separation will be developed by (1) establishing a rationale, (2) making the basic assumptions necessary to implement this rationale, and (3) performing the probabilistic development on the basis of the rationale and assumptions.

Rationale

In this development of a statistical model of ground scatterer separation, the clutter cell RCS is considered a random variable which is composed of the RCS of many elementary scatterers within the cell. Since the clutter cell is defined as the smallest resolvable ground patch, the cell RCS represents the contribution of all elementary scatterers in the cell which react within the constraints of the resolution of the radar. Therefore, in this study, the clutter cell size will be designated on the basis of some range resolution and some azimuth resolution, i.e., on the basis of the radar ground resolution cell. Consequently, cell RCS will be determined on the basis of the constructive and destructive interference between elementary scatterer reflections.

This interference is primarily a function of the scatterer separation in both range and azimuth. Consequently, a two-dimensional mathematical model of scatterer separation on the ground is required even

though the cell RCS at any instant is determined only as a function of the range separation of elementary scatterers.[1] The second spatial dimension is required to establish the rate of change of scatterer separation.

It will be subsequently shown that scatterer position within a cell is assumed to be random; consequently, scatterer separation within a cell will also be a random phenomenon since it is a function of scatterer position. Therefore, a statistical model of scatterer separation is required because of the random nature of scatterer separation.

Assumptions

The statistical model is based upon several rather general assumptions about the nature of terrain in terms of the elementary scatterers within a cell. These assumptions are as follows:

(1) The location of independent scatterers is characterized by a uniform random distribution.

(2) Scatterers are nondominant, isotropic, points.

(3) A cell contains a large number of scatterers.

Assumptions (1) and (3) are self-explanatory; nondominant, elementary scatterers are defined as those whose amplitudes are approximately equal. These assumptions are generally the same as, if not less restrictive than, the assumptions made by previous investigators (2). For example, Rihaczek (10) assumes, for purposes of clutter filtering, that ground clutter is derived from scatterers which are unresolvable, large

---

[1] On the assumption of equal return from each scatterer within the cell (except, of course, for phase).

in number, independent, uniformly distributed in range, randomly located, and of comparable length, and that such scatterers give rise to clutter with characteristics of stationary gaussian noise.

Although the assumptions made in this thesis in general tend to eliminate applications to the return from cities and man-made objects, at microwave frequencies even these man-made objects will generally exhibit an RCS made up of the returns from many separate scatter points. Therefore while these assumptions will degrade the usefulness of such a model in modeling man-made objects, the model is by no means completely inapplicable in these cases. However, the assumptions have been made for the primary purpose of modeling natural terrain which is of considerable interest in ground mapping by radar.

Development of Probability Density Function

By assumption, scatterers within a cell are characterized by a two-dimensional uniform distribution of position as shown in Figure 1 (Figure 2 will be shown to result from Figure 1). This two-dimensional probability density function (joint density function) shown in Figure 1 may be expressed as the product of the marginal probability density functions of X_1 and X_2, i.e.,

$$f_{\bar{X}}(\bar{x}) = f_{X_1}(x_1) f_{X_2}(x_2) = \left(\frac{1}{K_1}\right)\left(\frac{1}{K_2}\right) \qquad \text{for } 0 < x_1 < K_1,\ 0 < x_2 < K_2 \qquad (2.1)$$

$$= 0 \qquad \text{elsewhere} \quad .$$

Therefore X_1 and X_2 are independent random variables.

These two-dimensional position points may be considered random vectors. Then if two sample random vectors, $\bar{X}$ and $\bar{Y}$, are withdrawn at

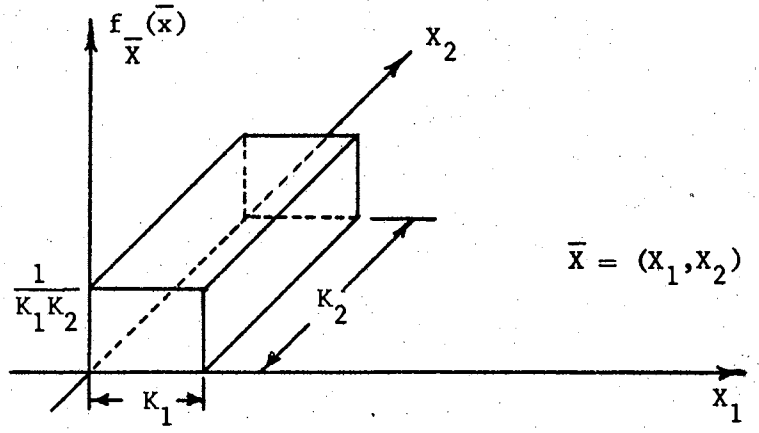

Figure 1. Probability Density Function of Scatterer Position

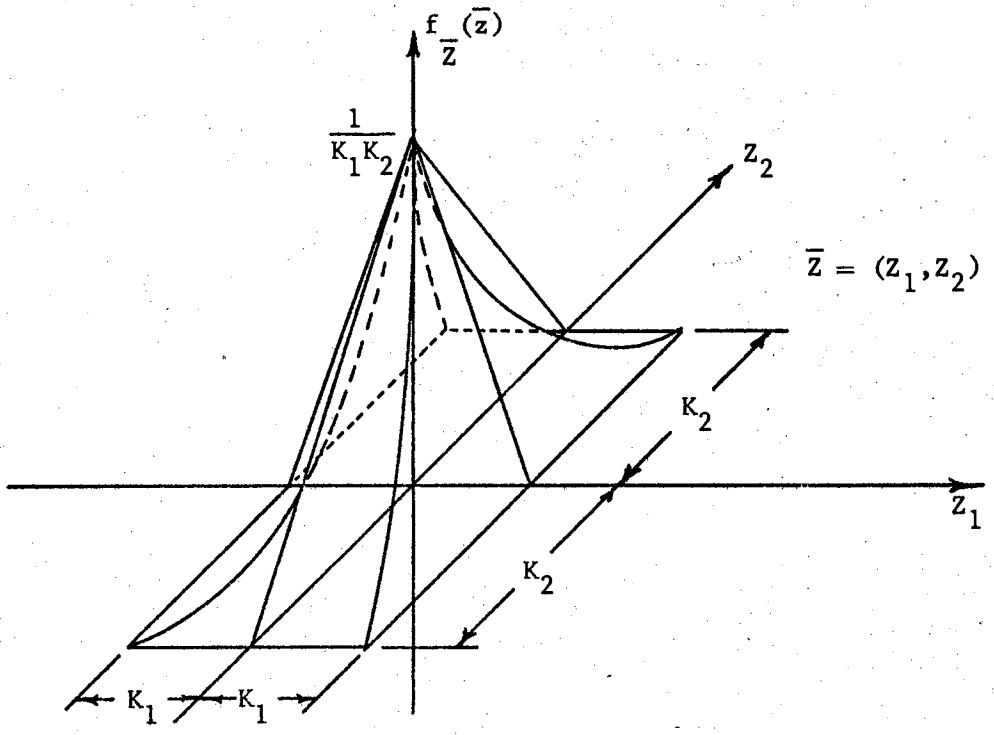

Figure 2. Probability Density Function of Scatterer Separation

random from this distribution, $\bar{X}$ and $\bar{Y}$ are independent, identically distributed random vectors. But the random vector of interest is the difference between $\bar{X}$ and $\bar{Y}$, which is

$$\bar{Z} = \bar{X} - \bar{Y} \tag{2.2}$$

where

$$Z_1 = X_1 - Y_1 \tag{2.3}$$

and

$$Z_2 = X_2 - Y_2 \quad . \tag{2.4}$$

Thus X_1 is independent of X_2 and Y_2, and Y_1 is independent of X_2 and Y_2 so Z_1 is independent of Z_2. It then follows that

$$f_{\bar{Z}}(z) = f_{Z_1}(z_1) f_{Z_2}(z_2) \quad , \tag{2.5}$$

but the density function of Z_1 is the convolution of the density of X_1 with $-Y_1$ (11, page 189) which is

$$\begin{aligned} f_{Z_1}(z_1) &= \int_{-\infty}^{\infty} f_{X_1}(z_1+y_1) f_{Y_1}(y_1) dy_1 \\ &= \frac{1}{K_1 K_2} (K_1 - |z_1|) \qquad \text{for } -K_1 < z_1 < K_1 \\ &= 0 \qquad\qquad\qquad\quad \text{elsewhere} \quad . \end{aligned} \tag{2.6}$$

Similarly

$$\begin{aligned} f_{Z_2}(z_2) &= \frac{1}{K_1 K_2} (K_2 - |z_2|) \qquad \text{for } -K_2 < z_2 < K_2 \\ &= 0 \qquad\qquad\qquad\quad \text{elsewhere} \quad . \end{aligned} \tag{2.7}$$

The combination of Equations 2.5, 2.6, and 2.7 results in the desired probability density function as shown in Figure 2. This density function is the statistical model of elementary scatterer separation expressed as a mathematical function. In terms of the components of the random vector $\bar{Z}$, this function becomes

$$f_{Z_1,Z_2}(z_1,z_2) = \frac{1}{K_1K_2}\left(1 - \frac{|z_1|}{K_1}\right)\left(1 - \frac{|z_2|}{K_2}\right) \qquad \text{for } -K_1 < z_1 < K_1,\ -K_2 < z_2 < K_2$$

$$= 0 \qquad \text{elsewhere} \tag{2.8}$$

where

z_1 = scatterer separation on the ground along the radius vector

z_2 = scatterer separation on the ground normal to the radius vector

K_1 = cell dimension in the z_1 direction

K_2 = cell dimension in the z_2 direction.

This function describes the basic randomness in the clutter process, and it will be used in conjunction with the deterministic model to describe the clutter process.

CHAPTER III

DETERMINISTIC MODEL BASED UPON GEOMETRY

A deterministic model, based upon geometry, is necessary for the description of the clutter process for the following reasons. The clutter process is to be modeled in terms of aircraft motion since it is aircraft motion which gives rise to the time variation. The separation of scatterers has been described statistically; however, it is the phase difference between scatterers, a function of scatterer separation, which determines the interference phenomenon. Therefore, phase difference and rate of change (first derivative) of phase difference, with respect to distance along ground track, will be described in terms of aircraft motion and of the Z_1 and Z_2 components of the random vector for scatterer separation. The model of the geometric relationships is presented in Figure 3.

The symbols and notation used in the model are described in the following list:

r = slant range to scatterer

Δr = slant range separation between scatterers

ground track = path of aircraft projected onto the ground

u = distance along ground track

$\dot{u}$ = aircraft velocity along ground track

v = distance normal to ground track

h = aircraft altitude

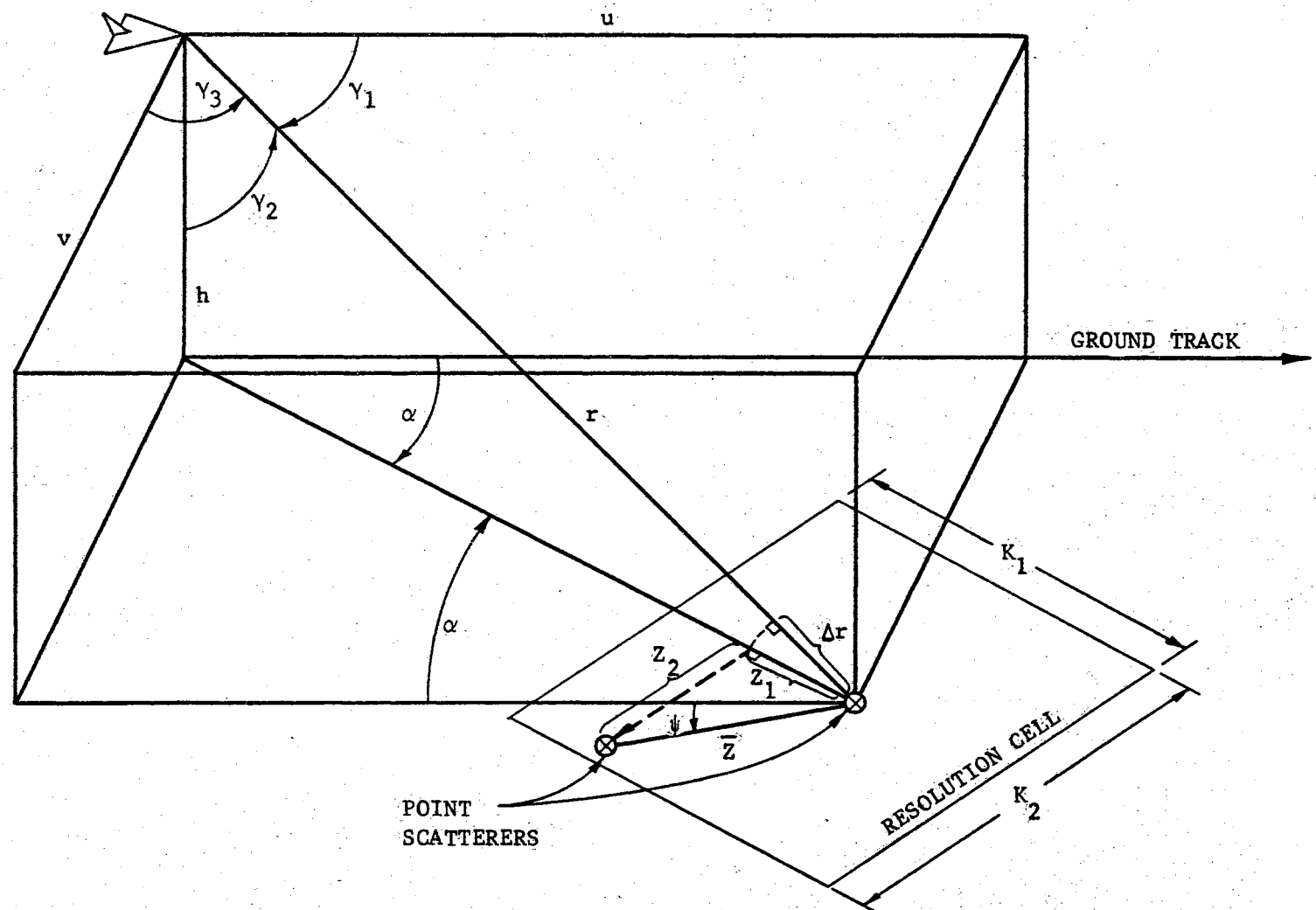

Figure 3. Geometric Model

$\gamma_1, \gamma_2, \gamma_3$ = direction angles to resolution cell

α = azimuth angle to resolution cell

c = propagation velocity of an electromagnetic wave

τ = radar pulse width

$\Delta\theta$ = phase difference between two scatterers

λ = wavelength

φ = antenna horizontal beamwidth

$K_1 = \frac{c\tau}{2} \csc \gamma_2$, i.e., range resolution

$K_2 = r\varphi$, i.e., azimuth resolution.

Assumptions

The geometric model shown in Figure 3 is the model generally used for the solution of the radar problem. However, three assumed approximations are inherent in this traditionally used model. First, it is assumed that range resolution is determined solely by pulse width and depression angle and not vertical beamwidth (i.e., large vertical beamwidth). For most practical purposes, use of this approximation causes no discernable error at ground range distances larger than aircraft altitude, but a model based on this approximation cannot be used when radars gather data from the ground at near vertical incidence, e.g., radar altimeters and some doppler radars. Second, it is assumed that the resolution cell in this model is a rectangular rather than an annular-section resolution cell. Since small horizontal beamwidths are used on most airborne radars, use of this approximation causes negligible error. Third, this model is based on the assumption that Earth is flat (but not smooth).

Development of Geometric Relationships

The geometric model is made up of two coordinate systems. The first is a three-dimensional coordinate system at the aircraft and it is translating at aircraft velocity. This coordinate system is used to designate cell position. The second is a two-dimensional coordinate system on the ground, and it is rotating (but not translating) as a result of aircraft motion. This coordinate system is used to designate scatterer position within a cell. A study of the above relationships will indicate that, in essence, only one cell on the ground is being tracked. In other words, a ground cell is being observed from a moving platform, and at each observation instant the cell coordinate system remains aligned with the azimuth angle from the moving observation platform to the cell.

Phase of the return from a scatterer is determined at any instant by the slant range to the scatterer, where slant range is expressed in terms of the geometric relationships discussed above. Therefore phase difference between two scatterers at any instant may be described in terms of the difference in their slant ranges. But from one instant of time to the next, phase difference changes as a result of the change in geometric relationships caused by aircraft motion. It is phase difference and change in phase difference which cause cell RCS variations as a function of change in position of the aircraft.

Thus phase difference and the change in phase difference will be determined in terms of the random variables Z_1 and Z_2 and the coordinates of cell position with respect to the aircraft. Two-way phase difference between two scatterers is given by 4π times range separation in wavelengths or

$$\Delta\theta = \frac{4\pi\Delta r}{\lambda} \tag{3.1}$$

where

$$\Delta r = Z_1 \sin \gamma_2 \quad . \tag{3.2}$$

Then expressing Z_1 in terms of $|\bar{Z}|$ and ψ, and expressing sin γ_2 in terms of u and v allows

$$\Delta r = |\bar{Z}|\left[\frac{u \cos\psi + v \sin\psi}{r}\right] \quad .$$

The change in $\Delta\theta$ with respect to u then is

$$\frac{d\Delta\theta}{du} = \frac{4\pi|\bar{Z}|}{\lambda}\left[\frac{(v^2+h^2)\cos\psi + (uv)\sin\psi}{r^3}\right] \quad . \tag{3.3}$$

It may be noted that, if this derivative is taken with respect to time, the following relationships results:

$$\Delta f_D = \frac{1}{2\pi}\frac{d\Delta\theta}{du}\dot{u} \tag{3.4}$$

$$= \frac{2\dot{u}|\bar{Z}|}{\lambda}\left[\frac{(v^2+h^2)\cos\psi + (uv)\sin\psi}{r^3}\right] \quad .$$

Then Δf_D is the difference in doppler frequency between the two scatterers. Equation 3.3 could have been derived by starting with the doppler frequency of each of two separated scatterers.

A coordinate transformation can be used to perform the operation necessary to obtain the $\bar{Z}$ values in terms of the random variables Z_1 and Z_2. It can be seen from Figure 3 that

$$Z_1 = |\bar{Z}| \cos(\psi + \alpha)$$

$$Z_2 = |\bar{Z}| \sin(\psi + \alpha) \quad . \tag{3.5}$$

Then by using the double angle trigonometric identities and converting Equation 3.5 to matrix form, the following is obtained,

$$\begin{bmatrix} Z_1 \\ Z_2 \end{bmatrix} = A \begin{bmatrix} |\bar{Z}| \cos\psi \\ |\bar{Z}| \sin\psi \end{bmatrix} \tag{3.6}$$

where

$$A = \begin{bmatrix} \cos\alpha & -\sin\alpha \\ \sin\alpha & \cos\alpha \end{bmatrix} \tag{3.7}$$

and

$$A^{-1} = \begin{bmatrix} \cos\alpha & \sin\alpha \\ -\sin\alpha & \cos\alpha \end{bmatrix} \quad .$$

It then follows that

$$\begin{bmatrix} |\bar{Z}| \cos\psi \\ |\bar{Z}| \sin\psi \end{bmatrix} = A^{-1} \begin{bmatrix} Z_1 \\ Z_2 \end{bmatrix}$$

or

$$|\bar{Z}| \cos\psi = Z_1 \cos\alpha + Z_2 \sin\alpha \tag{3.8}$$

$$|\bar{Z}| \sin\psi = -Z_1 \sin\alpha + Z_2 \cos\alpha \quad . \tag{3.9}$$

Applying relationships 3.8 and 3.9 to Equation 3.3 and combining Equations 3.1 and 3.2 produce

$$\Delta\theta = \frac{4\pi \sin\gamma_2}{\lambda} Z_1 \tag{3.10}$$

$$\frac{d\Delta\theta}{d\,u} = \frac{4\pi}{\lambda} \left[\frac{uh^2}{r^3\sqrt{u^2+v^2}} Z_1 + \frac{v}{r\sqrt{u^2+v^2}} Z_2 \right] \quad . \tag{3.11}$$

Equations 3.10 and 3.11 are the desired relationships and represent the deterministic model in terms of the random variables Z_1 and Z_2. These equations may be written as

$$\Delta\theta = aZ_1 = \frac{4\pi \sin\gamma_2}{\lambda} Z_1 \tag{3.12}$$

$$\frac{d\Delta\theta}{d\,u} = d_1 Z_1 + d_2 Z_2 \tag{3.13}$$

where

$$a = \frac{4\pi \sin\gamma_2}{\lambda}$$

$$d_1 = \frac{uh^2}{r^3\sqrt{u^2+v^2}} \left(\frac{4\pi}{\lambda}\right)$$

$$d_2 = \frac{v}{r\sqrt{u^2+v^2}} \left(\frac{4\pi}{\lambda}\right) \quad .$$

CHAPTER IV

STATE MODEL OF PROCESS

The model developed thus far does not incorporate a function of time. Time will be introduced by considering a discrete state model in the form of a first-order linear difference equation. Since the pulsed radar data sequence is generally accepted as Markov-1, such a state equation is sufficient for linear mean square estimation of the next value in the sequence in terms of all past values (11, page 420). This type of state model is readily applicable to many types of problems; in particular, the Kalman or Bayesian approach to recursive filtering may be applied through the use of the discrete state model.

The state model, along with the clutter autocorrelation function and other first-order and second-order moments developed in this chapter, will be considered the basic clutter model.

Development of the State Model

In order to apply the previously developed models in the development of the state model, clutter cell RCS must be described in terms which include the effect of the phase difference between scatterers. The effect of the phase difference can be described by obtaining the square of the resultant magnitude from the phasor addition of the square root of the RCS of many independent scatterers (see Appendix C).

Let σ designate cell RCS and σ_i designate the RCS of elementary

scatterer i within the cell; then consider

$$(\sigma)^{\frac{1}{2}} e^{j(\omega t+\theta)} = \sum_{i=1}^{N} (\sigma_i)^{\frac{1}{2}} e^{j(\omega t+\theta_i)} \tag{4.1}$$

where

N = number of elementary scatterers in the cell

θ_i = phase of elementary scatterer i.

Equation 4.1 is the phasor addition of the square root of elementary scatterer RCS, and $e^{j\omega t}$ may be factored from each side of Equation 4.1. Therefore,

$$(\sigma)^{\frac{1}{2}} e^{j\theta} = \sum_{i=1}^{N} (\sigma_i)^{\frac{1}{2}} e^{j\theta_i} \tag{4.2}$$

$$= \sum_{i=1}^{N} (\sigma_i)^{\frac{1}{2}} (\cos\theta_i + j \sin\theta_i)$$

$$= \sum_{i=1}^{N} (\sigma_i)^{\frac{1}{2}} \cos\theta_i + j \sum_{i=1}^{N} (\sigma_i)^{\frac{1}{2}} \sin\theta_i \quad .$$

It may be noted that, if the central limit theorem is applied at this point, we obtain two gaussian random variables. When these variables are combined and subsequently expressed only in terms of the resultant envelope, the Rayleigh distribution is obtained. This approach has been used by Downing (12, pages 51 through 59).

The following equation results from extracting only the magnitude from Equation 4.2:

$$(\sigma)^{\frac{1}{2}} = \left[\left(\sum_{i=1}^{N} (\sigma_i)^{\frac{1}{2}} \cos\theta_i\right)^2 + \left(\sum_{i=1}^{N} (\sigma_i)^{\frac{1}{2}} \sin\theta_i\right)^2\right]^{\frac{1}{2}} \qquad (4.3)$$

i.e., the square root of the sums of the square of the real and imaginary parts. Then squaring both sides and representing the squares as double sums result in

$$\sigma = \sum_{j=1}^{N} \sum_{k=1}^{N} (\sigma_j)^{\frac{1}{2}} (\sigma_k)^{\frac{1}{2}} \cos(\theta_k - \theta_j) \qquad (4.4)$$

or

$$\sigma = \sum_{j=1}^{N} \sum_{k=1}^{N} (\sigma_j)^{\frac{1}{2}} (\sigma_k)^{\frac{1}{2}} \cos\Delta\theta_{kj} \quad , \qquad (4.5)$$

where

$$\Delta\theta_{kj} = \theta_k - \theta_j \qquad (4.6)$$

is the phase difference between elementary scatterers as it has been defined in Equation 3.1.

By noting that Equation 4.5 is a quadratic form, it may be rewritten in matrix form as the following dot product:

$$\sigma = B \begin{bmatrix} \sigma_1^{\frac{1}{2}} \\ \sigma_2^{\frac{1}{2}} \\ \vdots \\ \sigma_N^{\frac{1}{2}} \end{bmatrix} \cdot \begin{bmatrix} \sigma_1^{\frac{1}{2}} \\ \sigma_2^{\frac{1}{2}} \\ \vdots \\ \sigma_N^{\frac{1}{2}} \end{bmatrix} \qquad (4.7)$$

where B is a square matrix of cosine terms, i.e.,

$$B = \begin{bmatrix} 1 & \cos\Delta\theta_{12} & \cos\Delta\theta_{13} & \cdots & \cos\Delta\theta_{1N} \\ \cos\Delta\theta_{21} & 1 & & & \cdot \\ \cos\Delta\theta_{31} & & \cdot & & \cdot \\ \vdots & & & \cdot & \cdot \\ \cos\Delta\theta_{N1} & \cdot & \cdot & \cdot & \cdot \end{bmatrix} \tag{4.8}$$

The summation required by Equation 4.5 or Equation 4.7 may be accomplished by first summing along the diagonal of B, then summing over the portion above the diagonal, and finally summing over the portion below the diagonal. Since the elementary scatterers are assumed to be approximately equal in amplitude, the diagonal summation is $N\sigma_i$ and the summation above the diagonal is

$$\sigma_i \sum_{\ell=1}^{\frac{N(N-1)}{2}} \cos\Delta\theta_\ell \quad .$$

However, since

$$\cos\Delta\theta_{kj} = \cos\Delta\theta_{jk}$$

B is symmetric and the summation above the diagonal is equal to the summation below the diagonal. Then by utilizing this symmetry of B and combining the sums, σ is represented as

$$\sigma = N\sigma_i + 2\sigma_i \sum_{\ell=1}^{\frac{N(N-1)}{2}} \cos\Delta\theta_\ell \quad . \tag{4.9}$$

Note that, if N = 2, then

$$\sigma = 2\sigma_i + 2\sigma_i \cos\Delta\theta$$

which is simply an expression of the law of cosines for equal amplitudes $(\sigma_i)^{\frac{1}{2}}$.

The expected value of σ may be obtained by expressing $\Delta\theta$ in terms of the random variable Z_1 (Equation 3.12), multiplying $\cos\Delta\theta$ times the marginal density function of Z_1, and integrating. Specifically, by letting E denote the operation of taking the expected value,

$$E[\sigma] = E[N\sigma_i + 2\sigma_i \sum_{\ell=1}^{\frac{N(N-1)}{2}} \cos\Delta\theta_\ell]$$

$$= N\sigma_i + 2\sigma_i \sum_{\ell=1}^{\frac{N(N-1)}{2}} E[\cos\Delta\theta_\ell] \quad . \tag{4.10}$$

It is shown in Appendix A that the expected value obtained in this manner is given by

$$E[\sigma] = N\sigma_i \tag{4.11}$$

and the mean squared value is given by

$$E[\sigma^2] = 2N^2\sigma_i^2 \quad . \tag{4.12}$$

By letting the subscript m denote a particular radar return pulse (i.e., time or aircraft position), then the difference in cell RCS from m-1 to m is given by

$$\sigma_m - \sigma_{m-1} = 2\sigma_i \sum_{\ell=1}^{\frac{N(N-1)}{2}} (\cos\Delta\theta_{\ell,m} - \cos\Delta\theta_{\ell,m-1}) \qquad (4.13)$$

$$= b_m \quad .$$

Therefore, the state model is

$$\sigma_m = \sigma_{m-1} + b_m \qquad (4.14)$$

and since $E[\sigma_m] = E[\sigma_{m-1}]$, then

$$E[b_m] = 0 \quad . \qquad (4.15)$$

However, the variance of b_m is required for most applications of this model.

Autocorrelation Function

In the development of the variance of b_m, a key term appears. This term must be considered as the correlation between cell RCS m and m-1, however, it will be shown that, by allowing the time (or position) difference between m and m-1 to vary, an autocovariance function, which corresponds to the correlation term, can be obtained.

The variance of b_m may be expressed as

$$E[b_m]^2 = 4\sigma_i^2 \, E\left[\sum_{\ell=1}^{\frac{N(N-1)}{2}} (\cos\Delta\theta_{\ell,m} - \cos\Delta\theta_{\ell,m-1})\right]^2 \qquad (4.16)$$

or represented as a double sum,

$$E[b_m]^2 = 4\sigma_i^2 E\left[\sum_{\ell=1}^{\frac{N(N-1)}{2}}\sum_{j=1}^{\frac{N(N-1)}{2}}(\cos\Delta\theta_{\ell,m}-\cos\Delta\theta_{\ell,m-1})(\cos\Delta\theta_{j,m}-\cos\Delta\theta_{j,m-1})\right]$$

$$= 4\sigma_i^2 E\left[\sum_{\ell=1}^{\frac{N(N-1)}{2}}\sum_{j=1}^{\frac{N(N-1)}{2}}(\cos\Delta\theta_{\ell,m}\cos\Delta\theta_{j,m}+\cos\Delta\theta_{\ell,m-1}\cos\Delta\theta_{j,m-1}\right.$$

$$\left. - \cos\Delta\theta_{\ell,m-1}\cos\Delta\theta_{j,m}-\cos\Delta\theta_{\ell,m}\cos\Delta\theta_{j,m-1})\right] .$$

However, since $\Delta\theta_\ell$ is independent of $\Delta\theta_j$, all terms in the above sum are zero, except in the case of $\ell = j$. In this case, a single sum is obtained,

$$E[b_m^2] = 4\sigma_i^2 E\left[\sum_{k=1}^{\frac{N(N-1)}{2}}(\cos^2\Delta\theta_{k,m}+\cos^2\Delta\theta_{k,m-1}-2\cos\Delta\theta_{k,m}\cos\Delta\theta_{k,m-1})\right] . \quad (4.17)$$

Then by applying Equation 3.13 (the derivative of $\Delta\theta$ with respect to u), $\Delta\theta_{k,m}$ may be approximated in terms of $\Delta\theta_{k,m-1}$ by

$$(\Delta\theta_{k,m} - \Delta\theta_{k,m-1}) = \frac{d\Delta\theta_{k,m-1}}{du}\,\Delta u \quad (4.18)$$

$$= (d_1 Z_1 + d_2 Z_2)\Delta u = \delta_m$$

where Δu is distance traveled between samples m-1 and m. When Equation 4.18 is used and the necessary integration is effected, it is shown in

Appendix B that

$$E[\cos^2\Delta\theta_{k,m}] = E[\cos^2\Delta\theta_{k,m-1}] = \frac{1}{2} \tag{4.19}$$

and

$$E[b_m]^2 = 2N^2\sigma_i^2 - 2N^2\sigma_i^2 r_m = 2N^2\sigma_i^2[1-r_m] \tag{4.20}$$

where r_m is the correlation coefficient (or normalized covariance) between σ_m and σ_{m-1}. Then, because $E[\sigma_m] = E[\sigma_{m-1}]$

$$\begin{aligned} Var[b_m] = E[\sigma_m - \sigma_{m-1}]^2 &= E[\sigma_m^2 + \sigma_{m-1}^2 - 2\sigma_m\,\sigma_{m-1}] \\ &= 2E[\sigma_m^2] - 2E[\sigma_m\,\sigma_{m-1}] \end{aligned} \tag{4.21}$$

and by using Equations 4.12, 4.13, 4.20, and 4.21,

$$E[\sigma_m\,\sigma_{m-1}] = N^2\sigma_i^2(1 + r_m) \quad . \tag{4.22}$$

If the time (or distance traveled) from sample m-1 to sample m is allowed to vary, Equation 4.22 becomes the autocorrelation function of cell RCS. However, a more basic function is the autocovariance function which is Equation 4.22 after the squared mean value is removed, i.e., $N^2\sigma_i^2 r_m$. This is the autocovariance of σ_m. Thus the function developed in Appendix B as a function of distance traveled by the aircraft (rather than time) is the normalized autocovariance function of σ_m as defined by Downing (12, page 25) and is given by

$$r_m(u,v,\Delta u) = \left[\frac{\sin\frac{d_1K_1\Delta u}{2}}{\frac{d_1K_1\Delta u}{2}} \; \frac{\sin\frac{d_2K_2\Delta u}{2}}{\frac{d_2K_2\Delta u}{2}} \right]^2 \quad . \tag{4.23}$$

The constants d_1, d_2, K_1 and K_2 were defined in Chapter III. This function will be subsequently analyzed in Chapter V where it will be shown that r_m is a slowly varying function of u at aircraft velocities. This slow variation substantiates the validity of short-term stationarity.

The variance of b_m is given by Equation 4.20 as

$$S_m^2 = E[b_m^2] = 2N^2\sigma_i^2(1-r_m) \tag{4.24}$$

and the autocovariance of σ_m is given by

$$R_m = N^2\sigma_i^2 r_m \quad . \tag{4.25}$$

At this point it may be seen that the state model given in Equation 4.14 may be put in a more general form as

$$E[\sigma_m] = E[\sigma_{m-1}] \tag{4.26}$$

$$\sigma_m = E[\sigma_m] + v_m \quad . \tag{4.27}$$

Cell radar cross section then is seen, from Equation 4.27 to be a random process consisting of a mean value and a correlated fluctuation component designated by v_m. This correlated noise component is the term which has been called clutter, and it is seen that RCS autocovariance is clutter autocorrelation, or since the clutter has a zero mean, clutter autocovariance is the same as clutter autocorrelation. Thus the zero mean clutter process will be referred to as RCS clutter or simply clutter while the nonzero mean RCS process, which consists of mean RCS plus clutter, will be referred to as RCS or RCS process.

The time state model will be applied in a Bayesian approach to recursive filtering of ground clutter in Chapter VII.

Scan-to-Scan Clutter Variance

The clutter correlation phenomenon discussed above is also reflected in scan-to-scan clutter variance. It will be shown that as pulse-to-pulse clutter correlation increases, scan-to-scan variance increases and increased scan-to-scan variance produces increased clutter. (This increased clutter can be identified in the presentations generally seen on airborne displays.) The significant conclusion is that increase in clutter can therefore be directly equated with an increase in pulse-to-pulse clutter correlation.

As in Appendix B, the assumption is made that the density function $f_{Z_1,Z_2}(z_1,z_2)$ does not change during one scan time, i.e., short term stationarity. Then, if it is assumed that n hits per scan are summed (or integrated) by the radar and M is used as a scan-to-scan index subscript and m as a pulse-to-pulse index subscript as before, the scan-to-scan cell RCS is given by

$$\sigma_M = \frac{1}{n} \sum_{m=1}^{n} \sigma_m \quad . \tag{4.28}$$

This equation represents the uniformly weighted sum of n correlated identically distributed samples. The expected value is given by

$$E[\sigma_M] = \frac{1}{n} [n\ E(\sigma_m)]$$

$$= N\ \sigma_i \quad . \tag{4.29}$$

Then

$$E[\sigma_M^2] = E[\frac{1}{n} \sum_{m=1}^{n} \sigma_m]^2$$

$$= \frac{1}{n^2} \sum_{m=1}^{n} \sum_{\ell=1}^{n} E[\sigma_m \sigma_\ell] \quad . \tag{4.30}$$

By using Equation 4.22 for $E[\sigma_m \sigma_\ell]$,

$$E[\sigma_M^2] = N^2\sigma_i^2 + \frac{1}{n^2} \sum_{m=1}^{n} \sum_{\ell=1}^{n} N^2\sigma_i^2 r_{\ell,m}(\ell-m) \tag{4.31}$$

and the variance of σ_M is given by

$$E[\sigma_M^2] - N^2\sigma_i^2 = \frac{1}{n^2} \sum_{m=1}^{n} \sum_{\ell=1}^{n} R_{\ell,m}(\ell-m) \quad . \tag{4.32}$$

The double summation may be represented in matrix form as

$$C = \begin{bmatrix} R(0) & R(1) & R(2) & . & . & R(n-1) \\ R(1) & R(0) & R(1) & & & . \\ R(2) & R(1) & R(0) & & & . \\ . & & & & & \\ . & & & & & R(2) \\ . & & & & & R(1) \\ R(n-1) & . & . & R(2) & R(1) & R(0) \end{bmatrix} . \tag{4.33}$$

Then by summing C on the diagonal, the variance of σ_M is obtained as

$$Var[\sigma_M] = \frac{N^2\sigma_i^2}{n^2} [n + 2 \sum_{k=1}^{n-1} (n-k)r_k(k)] \tag{4.34}$$

which is similar to the relation developed by Costas (13, page 5).

It may be noted that, if pulse-to-pulse correlation $r_k(k)$ is zero, then scan-to-scan variance is equal to the pulse-to-pulse variance divided by n, $(N^2\sigma_i^2/n)$, as expected, and clutter is reduced by a factor of 1/n, which is the same reduction obtained through the integration of white noise. When pulse-to-pulse correlation is complete ($r_k(k) = 1$ for all $k \leq n$), scan-to-scan variance is the same as pulse-to-pulse variance (i.e., the integration is not effective in smoothing), and the resulting high clutter is reflected on the radar display. Thus a large pulse-to-pulse correlation tends to cancel the smoothing provided by integration. Consequently a large scan-to-scan variance, i.e., the noise-like modulation called clutter, is obtained. Of course, scan-to-scan integration will smooth this clutter, but it will also degrade the time resolution of the radar. A similar smoothing could be obtained by cell-to-cell integration, but this action would degrade the space resolution of the radar.

CHAPTER V

AUTOCORRELATION FUNCTION ANALYSIS

Analysis of the autocorrelation function is directed to identifying the variant and invariant properties of the function. This identification, in turn, is dependent on examining the function by means of three-dimensional plots of the function itself and its Fourier transform. This analysis is also dependent on a knowledge of the specific parameters of the function. The autocorrelation function given by Equation 4.23 is a function of distance along ground track, u, distance normal to ground track, v, and difference distance along ground track, Δu (Figure 3). The parameters of this function are pulse width, beamwidth, wavelength, and altitude which could also be considered variable.

The term correlation is somewhat ambiguous in that it may refer to amplitude or width (distance in wavelengths) of the normalized clutter autocorrelation function. However, the area under the autocorrelation function curve is a better measure of the quantity of interest than either amplitude or width, but the area is essentially a direct function of the width (or correlation distance) since the basic shape of the curve will be shown not to vary appreciably from a linear function. Consequently, correlation distance will be considered the basic correlation parameter, and the term correlation will subsequently be used to refer to either area under the curve or correlation distance, interchangeably. The distance to the first point where the correlation

function touches the zero axis will be considered as the decorrelation distance.

It should be noted that this autocorrelation function is the autocovariance function of clutter RCS and not clutter voltage. Therefore, the Fourier transform of this function gives the power squared density spectrum which is the video spectrum actually seen on a radar only if a square law detector is used. It is not clear whether the RCS (analogous to power) or voltage spectrum is more basic; however, the RCS spectrum was chosen for reasons of mathematical tractability. Certainly the RCS autocovariance function provides valid clutter information although the voltage autocovariance provides the information in a form more generally accepted. A brief comparison of the difference between the two is presented in Appendix C.

Presentation of Autocorrelation Function

An analysis of the autocorrelation function involves a presentation of the function in a form which allows a grasp of the variations present and the parameter dependency. Such a presentation is generally some form of graph; however, this function is four dimensional. Therefore, the function is plotted in a three dimensional graph, and either u, v, or azimuth angle, α, is held constant on each graph. Use of this convention provides a graph of correlation amplitude on the vertical scale, correlation distance on the horizontal scale, and either ground track distance, cross track distance, or azimuth angle into the paper (the third dimension).

A normalization of the wavelength dependency and a more compact graphical presentation are desirable for clarifying the graphs. An

inspection of Equation 4.23 reveals that λ may be removed from the constants d_1 and d_2 and coupled with Δu as $\Delta u/\lambda$; in each case distance can then be presented in terms of wavelengths.

Since a mathematical expression for the clutter spectrum (power squared spectrum) at the video level is desirable in the analysis, the Fourier transform of the clutter autocorrelation (or autocovariance) function has been developed in Appendix D. A scale change of the resulting transform was then effected to allow the spectrum to be normalized in terms of velocity and wavelength. The clutter spectrum may now be plotted in three dimensions with amplitude times velocity (in wavelengths) on the vertical scale, frequency per unit velocity per wavelength (normalized frequency) on the horizontal scale, and either ground track or cross track distance into the paper.

Because of the length and complications of the equations for the function and its transform, a computer program was written and utilized for the calculation of the function values and the transform of these values which were used in calculating the points subsequently represented in the plots. The program provides an output in tabular form of the three dimensional autocorrelation function and the three dimensional spectrum. The graphical results provide a basis for further analysis of the clutter process in the remaining sections of this paper.

The autocorrelation function is plotted in graph form either at points along or across track or at slant ranges along a constant azimuth angle. The equation of the normalized autocorrelation function and its Fourier transform are as follows:

Clutter Autocorrelation Function:

$$r(u,v,\Delta u) = \begin{bmatrix} \dfrac{\sin \dfrac{d_1 K_1 \Delta u}{2}}{\dfrac{d_1 K_1 \Delta u}{2}} & \dfrac{\sin \dfrac{d_2 K_2 \Delta u}{2}}{\dfrac{d_2 K_2 \Delta u}{2}} \end{bmatrix} \tag{5.1}$$

Fourier Transform of Autocorrelation Function:

$$\frac{\dot{u}}{\lambda} F(u,v,f_1) = \frac{1}{24(\alpha_1\beta_1)^2} \{2f_1^3 - (f_1+2\alpha_1)^3 - |f_1-2\alpha_1|^3 - (f_1+2\beta_1)^3 - |f_1-2\beta_1|^3$$

$$+ \frac{1}{2}\,[f_1+(\alpha_1+\beta_1)]^3 + \frac{1}{2}\,|f_1-(\alpha_1+\beta_1)|^3 + \frac{1}{2}\,|f_1+(\alpha_1-\beta_1)|^3$$

$$+ \frac{1}{2}\,|f_1-(\alpha_1-\beta_1)|^3\} \tag{5.2}$$

where

$$f_1 = \frac{f}{\dot{u}/\lambda}$$

$$\alpha_1 = \frac{uh^2}{r^3\sqrt{u^2+v^2}}\,K_1$$

$$\beta_1 = \frac{v}{r\sqrt{u^2+v^2}}\,K_2 \quad .$$

Therefore the autocorrelation function is the product of two $\frac{\sin^2 x}{x^2}$ type curves. However a comparison of d_1K_1 with d_2K_2 reveals that for typical radar parameters and for ranges greater than altitude d_1K_1 is several orders of magnitude less than d_2K_2, except at angles very near ground track. Therefore

$$\left[\frac{\sin\frac{d_1K_1\Delta u}{2}}{\frac{d_1K_1\Delta u}{2}}\right]^2 \cong 1 \qquad (5.3)$$

throughout a major portion of the region of interest and the autocorrelation function then in this region is given by

$$r(u,v,\Delta u) \cong \left[\frac{\sin\frac{d_2K_2\Delta u}{2}}{\frac{d_2K_2\Delta u}{2}}\right]^2 . \qquad (5.4)$$

Near ground track, however, d_1K_1 becomes larger than d_2K_2 and the expression in Equation 5.3 predominates. These observations are borne out in the graphs which follow.

The Fourier transform of a $\frac{\sin^2 x}{x^2}$ type expression has a triangular shape (11, page 340). Therefore the Fourier transform of Equation 5.1 can be shown to be the convolution of two triangular shapes (12, page 340). But throughout a major portion of the region of interest one of the triangular shapes obtained from the Fourier transform will be much more narrow than the other. The convolution then of a triangular shape with a "spike" produces a triangular shape. This is borne out by the triangular shaped spectrum plots which follow.

Parametric Dependency

The autocorrelation function is obviously directly dependent upon wavelength. It was therefore studied by considering difference distances, Δu, in terms of wavelength. Of the other three designated

parameters, altitude, beamwidth, and pulse width, only beamwidth has any substantial effect throughout the region of interest. This may be deduced by considering the values of

$$\frac{d_1 K_1 \Delta u}{2} = \left(\frac{2\pi h^2}{r^2\sqrt{u^2+v^2}} \cos\alpha\right)\left(\frac{c\tau}{2}\right)\left(\frac{\Delta u}{\lambda}\right) \tag{5.5}$$

and

$$\frac{d_2 K_2 \Delta u}{2} = \left(\frac{2\pi \sin\alpha}{r}\right)(r\varphi)\left(\frac{\Delta u}{\lambda}\right)$$

$$= (2\pi\varphi \sin\alpha)\left(\frac{\Delta u}{\lambda}\right) \quad . \tag{5.6}$$

Therefore for $r \gg h$ the expression in Equation 5.5 is very small and

$$\left[\frac{\sin\frac{d_1 K_1 \Delta u}{2}}{\frac{d_1 K_1 \Delta u}{2}}\right] \longrightarrow 1 \quad .$$

So only Equation 5.6 effects the autocorrelation and altitude and pulse width are not included in this expression. Thus, except in the region very near ground track, the autocorrelation function is invariant with altitude and pulse width.

Along ground track the expression in Equation 5.6 is zero since $\sin\alpha$ is zero. Therefore

$$\left[\frac{\sin\frac{d_2 K_2 \Delta u}{2}}{\frac{d_2 K_2 \Delta u}{2}}\right]^2 = 1$$

and

$$r(u,v,\Delta u) = \left[\frac{\sin \frac{d_1 K_1 \Delta u}{2}}{\frac{d_1 K_1 \Delta u}{2}} \right]^2$$

along ground track. Examination of Equation 5.5 then reveals that variation of τ with h^2 constant is equivalent to variation of h^2 with τ constant. So to examine this parametric variation along ground track, Equation 5.1 was plotted allowing τ to vary. This is shown in Figure 4. An examination of this graph reveals that lines of constant correlation amplitude, when projected onto the zero correlation amplitude plane, are inverse functions of τ (as might be expected since increasing τ decreases the abscissa of each curve). For example the correlation distance for a 0.5 correlation amplitude and 2 microsecond pulse width is 56 wavelengths while for a 4 microsecond pulse width this distance is 28 wavelengths. Then allowing h^2 to vary instead of τ it may be shown that correlation distance (or correlation) along ground track is an inverse function of h^2. Therefore correlation varies inversely with pulse width and inversely with altitude squared along ground track. However when range is much larger than altitude this dependency is overshadowed by near complete correlation (correlation distance very large) along ground track.

In the region from a few degrees off ground track to broadside the predominant correlation relationship is given in Equation 5.4. Therefore an examination of Equation 5.6 reveals that in this region correlation depends upon beamwidth, φ, and is invariant with altitude and pulse

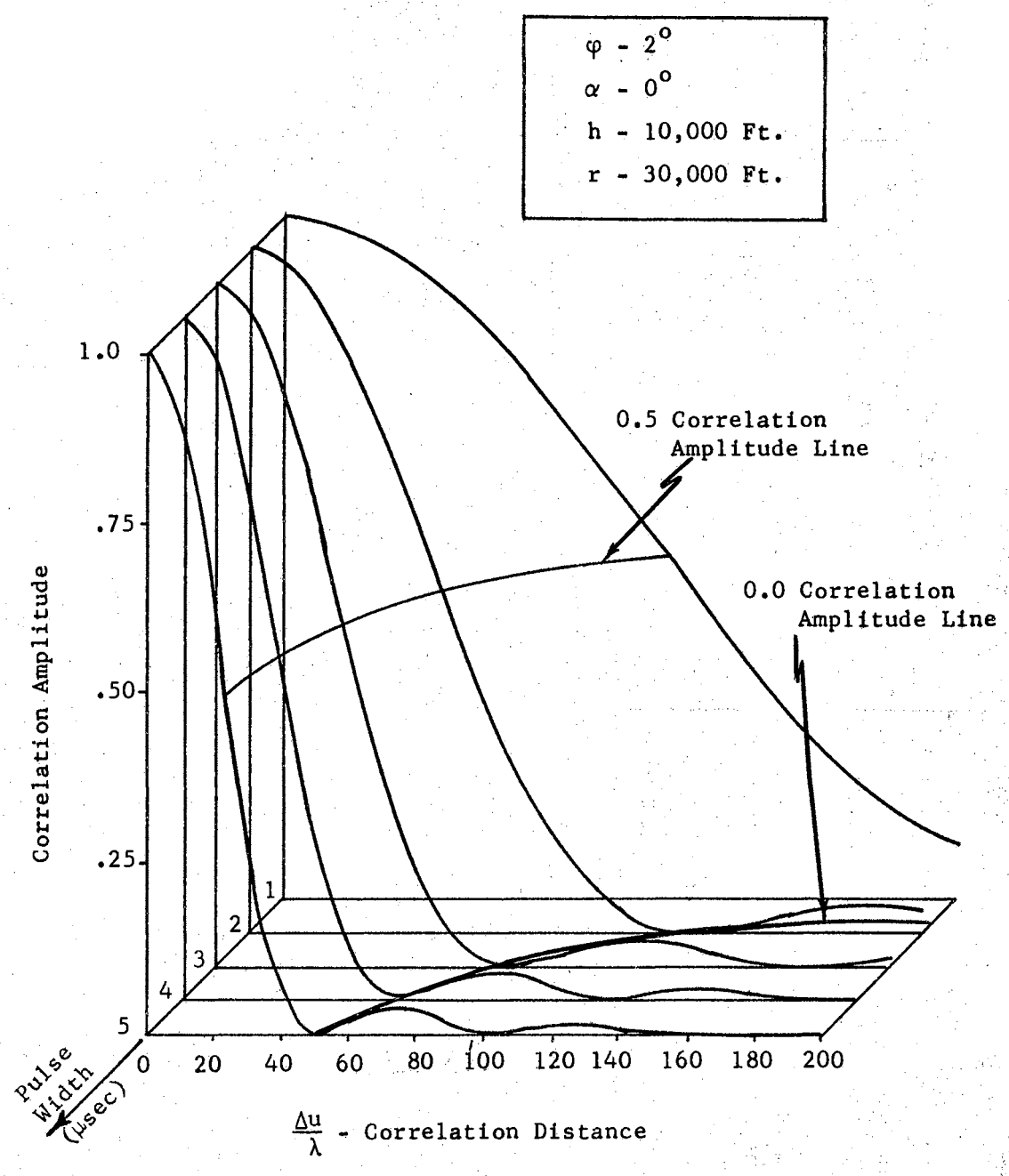

Figure 4. Autocorrelation Versus Pulse Width

width. As might be expected from the results above, correlation varies as an inverse function of φ. This is shown in Figure 5 for an azimuth angle of 45 degrees and is typical for all azimuth angles to within a few degrees of ground track for typical airborne radar parameters.

Geometric Dependency

The geometric dependency may be obtained in the same manner used above to obtain parametric dependency. Again an examination of Equations 5.4 and 5.6 reveals that correlation is invariant with range beyond some minimum range and at azimuth angles off ground track. Figure 6 shows the variation of the autocorrelation function with slant range at 15 degrees off ground track. As may be noted the function does not change with range beyond a slant range of two to three times altitude. As the azimuth angle increases the distance at which range becomes invariant shortens. For example at an azimuth angle of 90 degrees (broadside), range invariance begins when slant range (r) is only a few feet greater than altitude (i.e., at a ground range of a few feet).

By the arguments previously used then, correlation varies inversely with azimuth angle. This is shown in Figure 7. Figure 8 is a "blown-up" view of Figure 7 in the region from 15 degrees off ground track to ground track. An examination of Figure 8 reveals that the $\frac{1}{\sin\alpha}$ relationship holds very closely at angles as small as 2 degrees off ground track. Thus the basic shape of the autocorrelation function is invariant and its width varies inversely as the sine of the azimuth angle.

Since it may be necessary to track a particular clutter cell on the ground for filtering purposes, the clutter of interest is that along

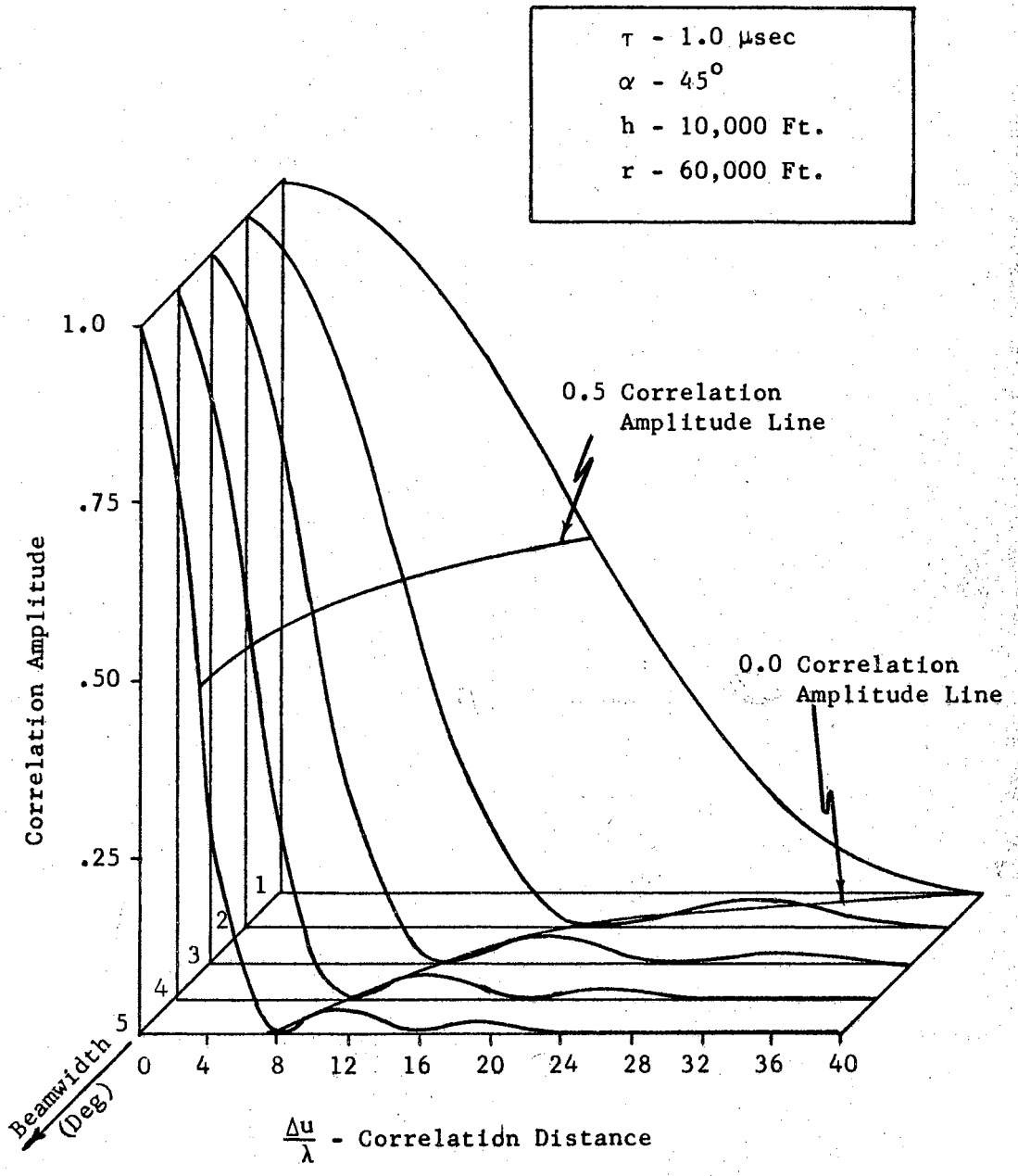

Figure 5. Autocorrelation Versus Beamwidth

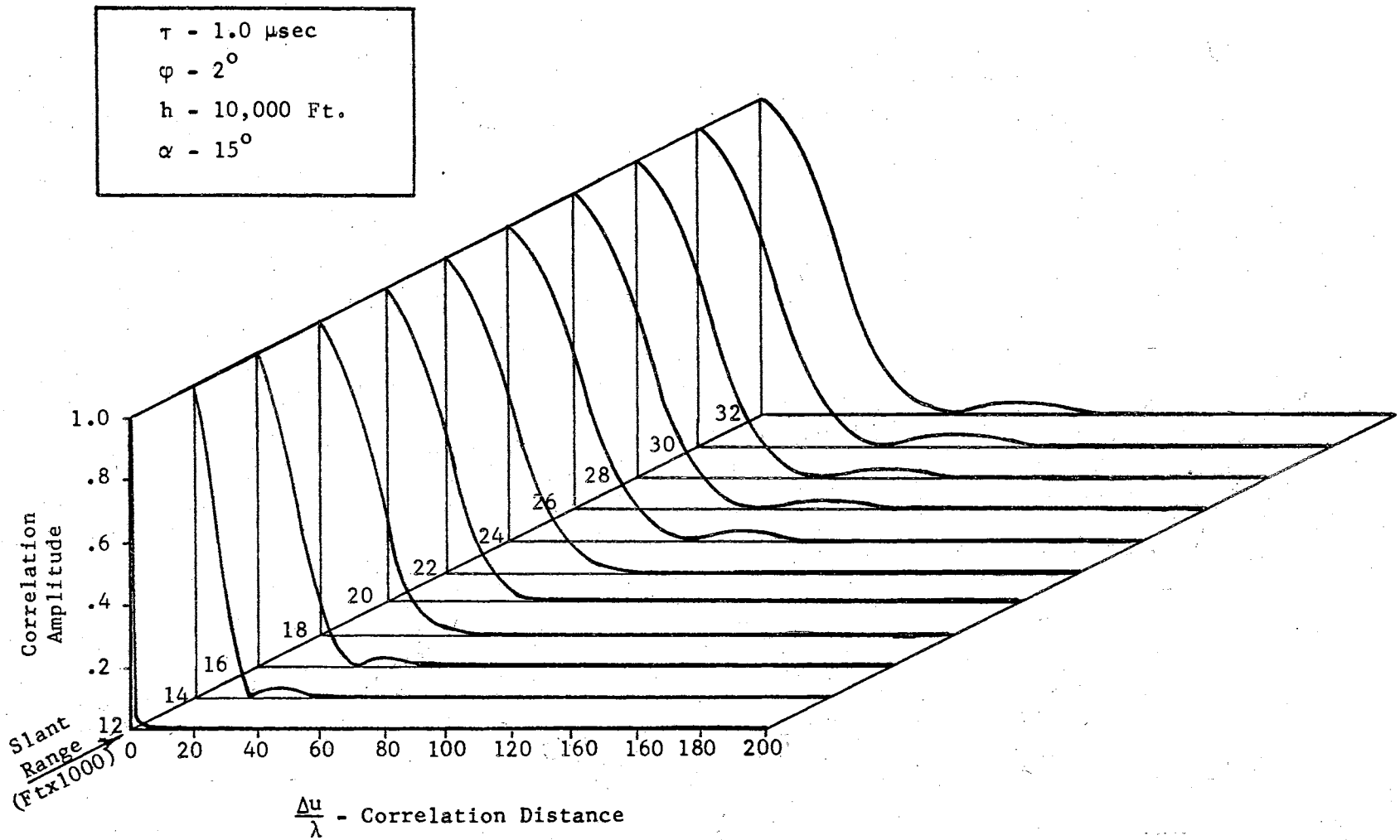

Figure 6. Autocorrelation at Short Range Along 15 Degree Azimuth

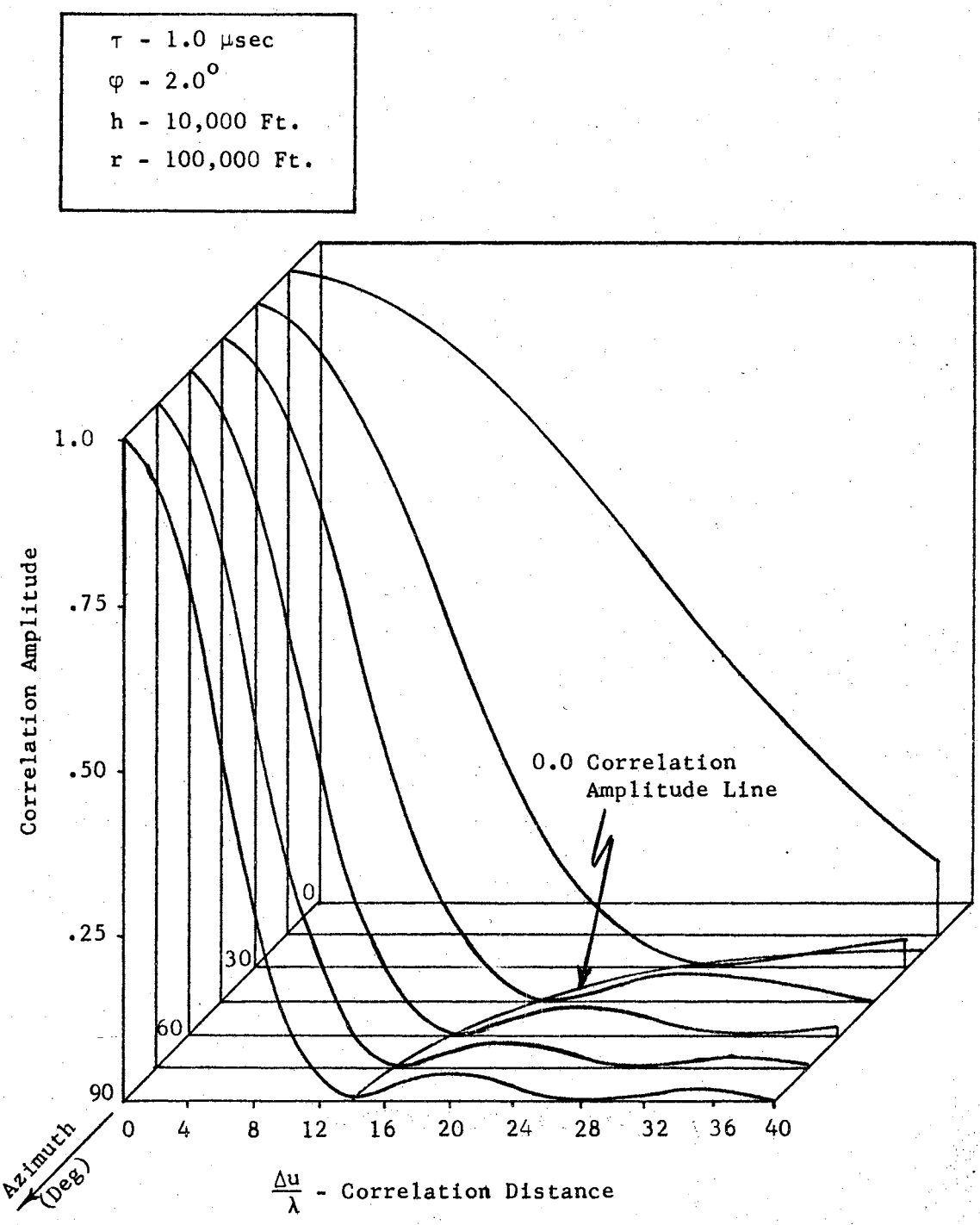

Figure 7. Autocorrelation Versus Azimuth

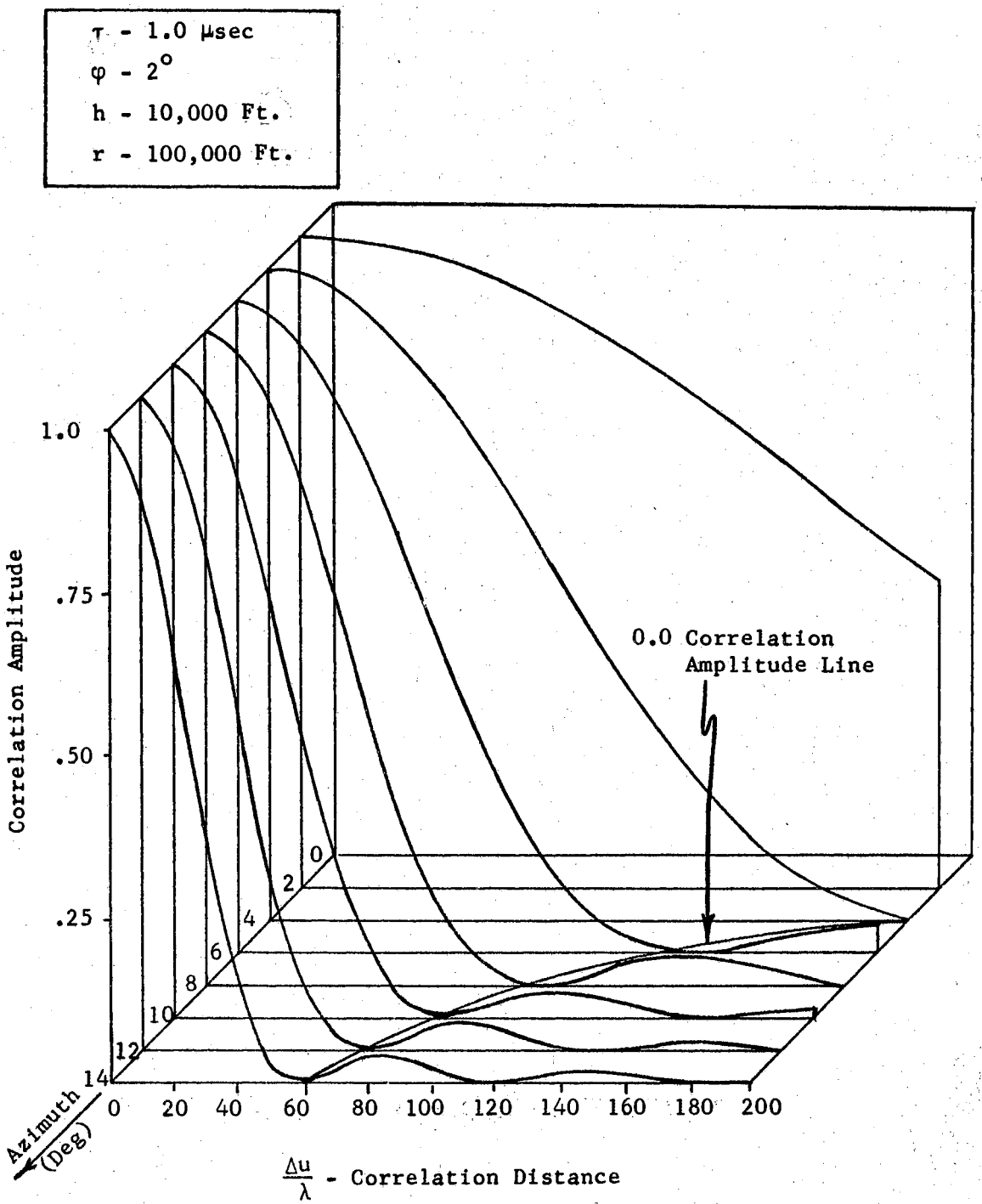

Figure 8. Autocorrelation Near Ground Track

a particular track parallel to ground track. For this reason clutter correlation and the clutter spectrum has been plotted along such a track as shown in Figures 9 and 10. Figures 11 and 12 are presented to show how the clutter correlation function and the clutter spectrum change with distance across track. Of course, the change noted in these figures results from the change in azimuth angle. It may be noted from Figures 9 and 11 that the autocorrelation function changes very slowly as a function of u or v in comparison with its change as a function of Δu.

The two spectrum graphs (Figures 10 and 12) verify several known relationships between the clutter autocorrelation function and the clutter spectrum. As the autocorrelation function becomes wider, i.e., as correlation is increased, the spectrum becomes narrower and higher in amplitude and more clutter is generally presented on the radar display. The spectrum shown in these figures is the video spectrum shifted to zero frequency (the doppler is removed); thus the spectrum width about the doppler frequency would be twice as wide as that shown in the graphs.

Clutter Correlation Characteristics

Some of the clutter RCS correlation characteristics may now be summarized on the basis of the discussion and an examination of the graphs presented. Examination reveals that the following approximate characteristics of correlation can be identified in the region off ground track:

(1) Correlation is invariant with range beyond some minimum range.

(2) Correlation is an inverse function of the sine of the azimuth

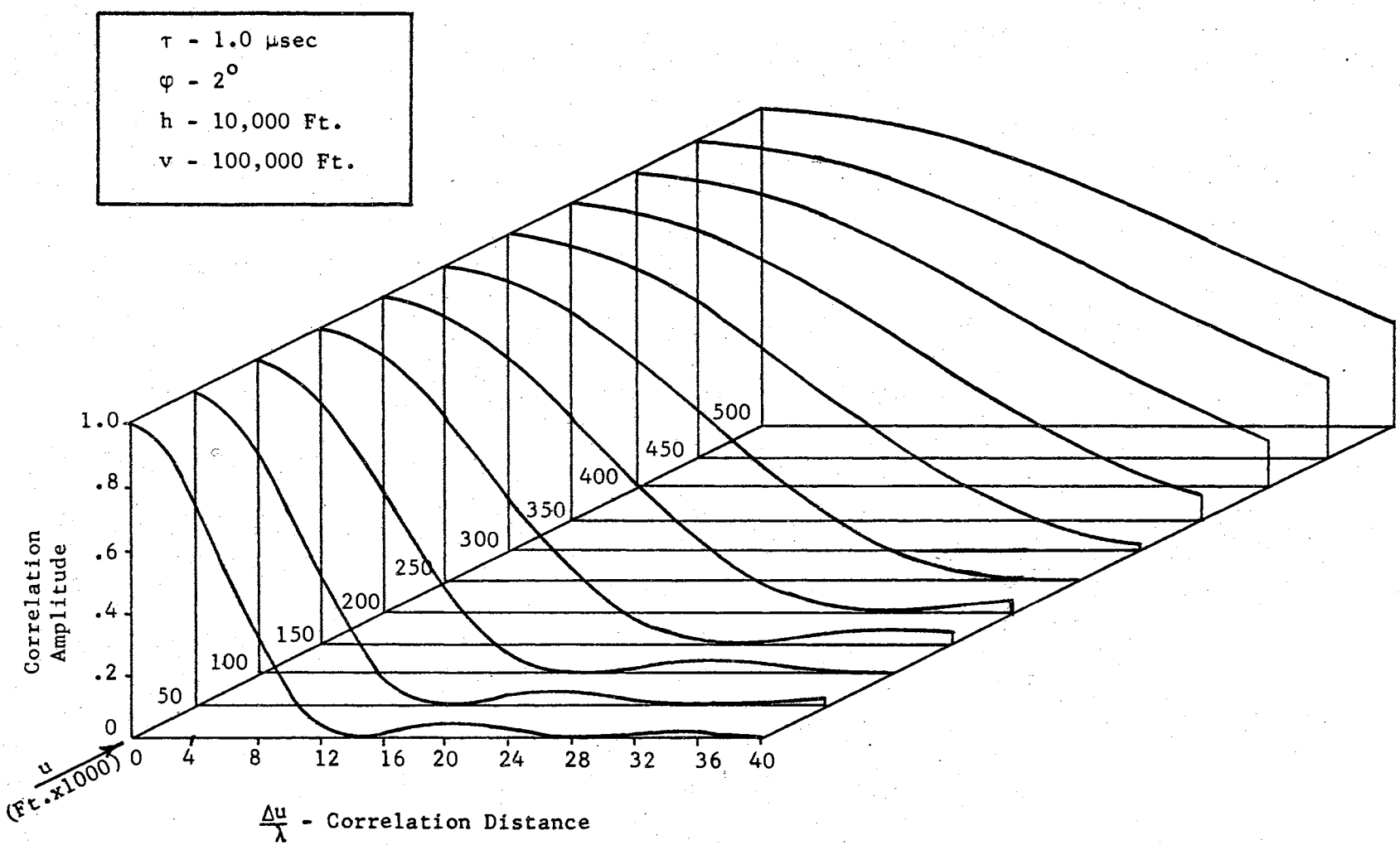

Figure 9. Autocorrelation Parallel to Ground Track

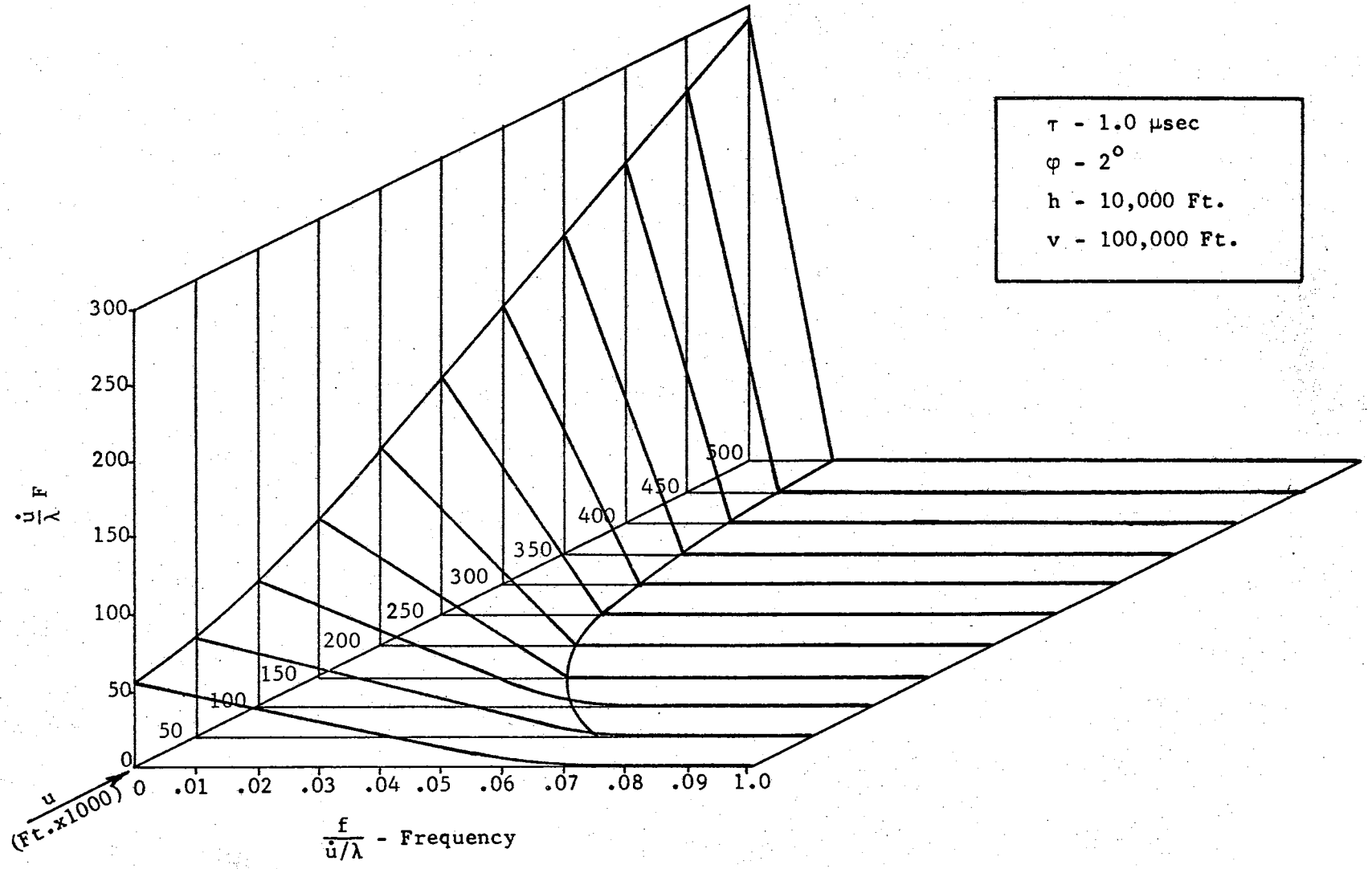

Figure 10. Spectrum Parallel to Ground Track

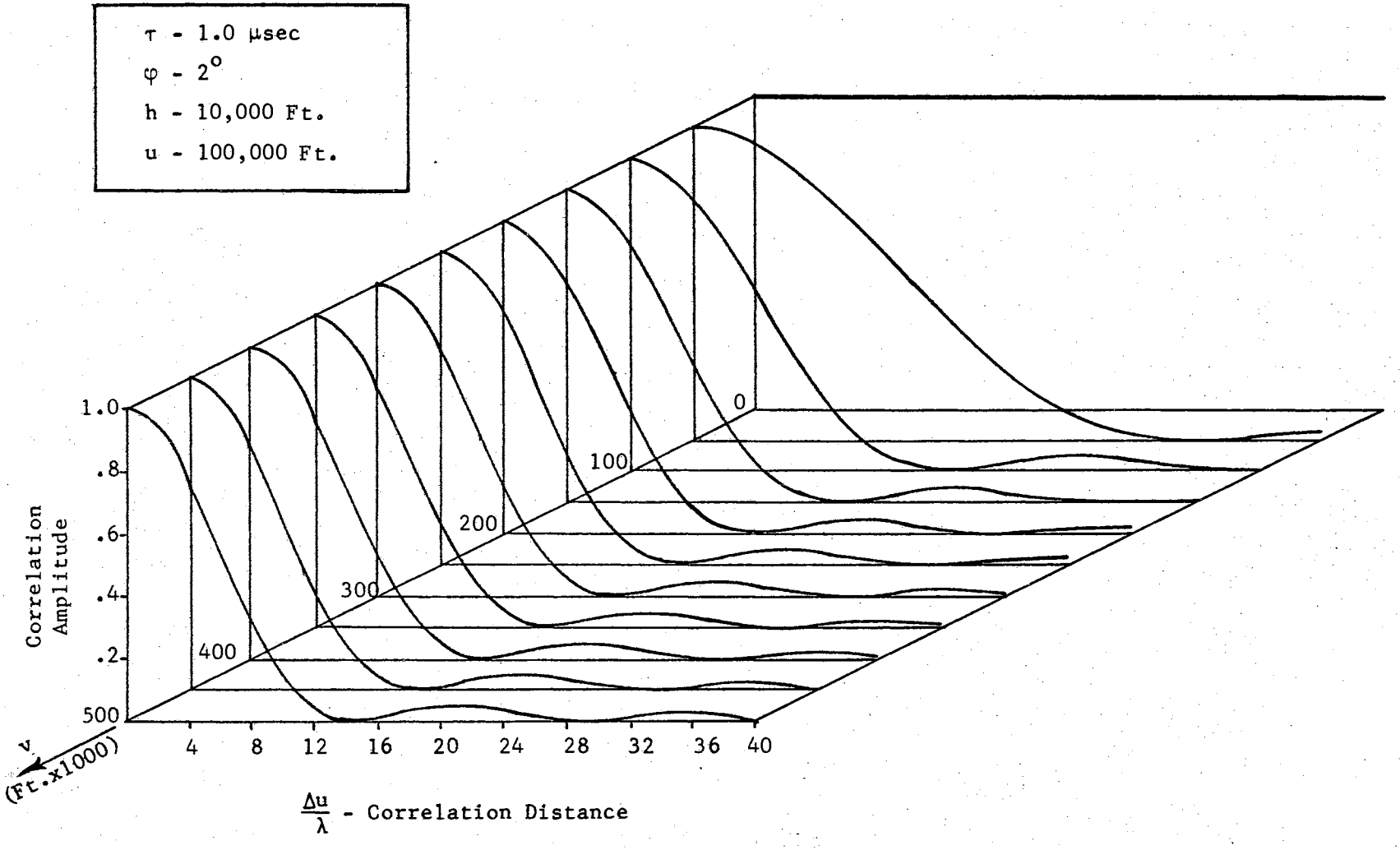

Figure 11. Autocorrelation Normal to Ground Track

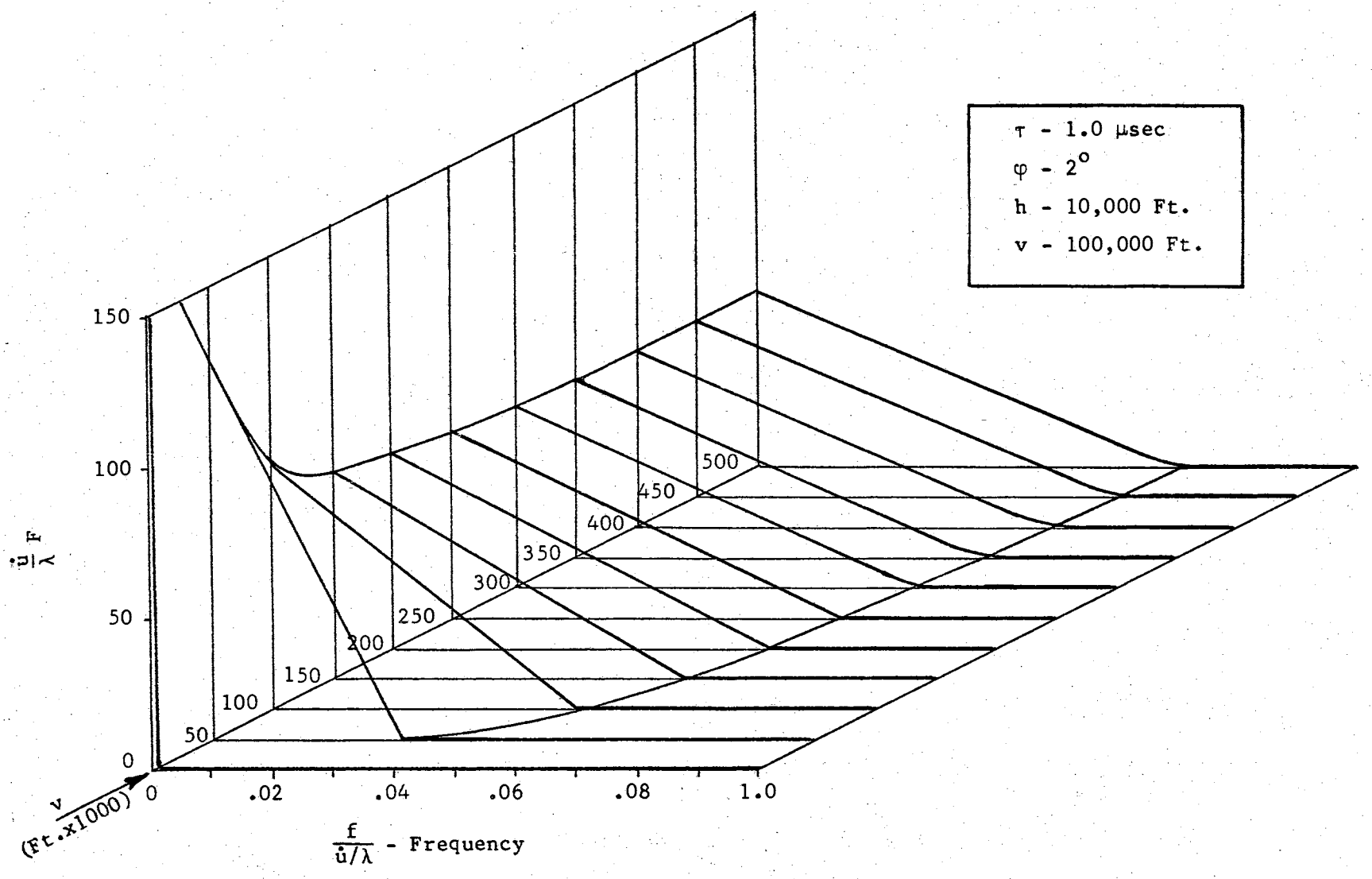

Figure 12. Spectrum Normal to Ground Track

angle and is thus maximum along ground track and minimum at 90 degrees off ground track.

(3) Correlation varies inversely with antenna beamwidth (verified in more detail in Chapter VI).

(4) At ranges greater than altitude, correlation is independent of altitude.

(5) Correlation is independent of pulse width.

(6) Correlation amplitude remains less than 0.05 after it is plotted through zero for the first time on any of the graphs.

(7) For typical airborne radar parameters the distance traveled by the radar between scans is greater than decorrelation distance (i.e., clutter uncorrelated scan to scan).

(8) Correlation is a direct function of wavelength. Approximately complete correlation is obtained along ground track.

Inspection of Equation 4.34 will indicate that, since clutter correlation is invariant with range, clutter increases with range only as a result of the clutter variance ($N^2\sigma_i^2$). It is shown in Appendix B that N is a function of slant range. However, at long ranges the effects of Earth curvature and the decrease in the ground reflection coefficient at small grazing angles tend to offset this increase. Neither of these parameters are considered in the model developed herein.

CHAPTER VI

AUTOCORRELATION FUNCTION RELATIONSHIPS

It was noted in Chapter V that the clutter autocorrelation function is essentially invariant in shape and that its most significant parameter is correlation distance. A simple expression for correlation distance in terms of aircraft motion and radar parameters is therefore desired because a known shape and known correlation distance can then be used to determine a value of pulse-to-pulse correlation at any ground position without a lengthy calculation of the autocorrelation function.

A condition generally desirable for radar is pulse-to-pulse decorrelation since it increases the information available per pulse. Therefore, the specific correlation distance to be determined will be referred to as decorrelation distance (d_c). This basic relationship is defined as the shortest distance at which the autocovariance function reaches the zero axis.

Decorrelation Distance

Decorrelation distance is found by determining the point where the autocorrelation function first reaches zero amplitude. The autocorrelation function reaches zero amplitude the first time when

$$\frac{d_2 K_2 \Delta u}{2} = \pi \tag{6.1}$$

for azimuth angles off ground track. Therefore applying the equations for d_2 and K_2 results in

$$(2\pi \sin\alpha)(\varphi)(\frac{\Delta u}{\lambda}) = \pi$$

or

$$\Delta u = \frac{\lambda}{2\varphi \sin\alpha} \quad . \tag{6.2}$$

But Δu in this case is the value defined as decorrelation distance and is designated as d_c. So converting φ to an angle in degrees

$$d_c = \frac{(57.3)(\lambda)}{2\varphi \sin\alpha} \quad . \tag{6.3}$$

Antenna beamwidth is a function of aperture width (D) and may be approximated by

$$\varphi = \frac{58\ \lambda}{D} \tag{6.4}$$

if a circular aperture illumination distribution is assumed. By using Equation 6.4 in Equation 6.3 above

$$d_c \cong \frac{D}{2 \sin\alpha} \quad . \tag{6.5}$$

Therefore decorrelation distance depends only on antenna size and azimuth angle and is independent of wavelength. This Equation 6.5 is the simple relationship desired.

Equation 6.5 was checked at azimuth angles as close as 2 degrees to ground track for typical airborne radar parameters and geometry and found to be accurate. However as the azimuth angle gets very small

(i.e., "on ground track") $\sin(d_1 K_1 \Delta u/2)/(d_1 K_1 \Delta u/2)$ predominates as noted in Chapter 5 and Equation 6.5 becomes invalid.

Autocorrelation Function Approximation

Since the basic shape of the autocorrelation function is invariant, an approximation to this shape could save considerable calculation in some applications without severe degradation of the accuracy. A linear approximation to the normalized autocorrelation function is shown in Figure 13 to be a reasonable approximation and is given by

$$r_m \cong 1 - \frac{\Delta d}{d_c} \qquad \text{for } \Delta d < d_c$$

$$\cong 0 \qquad \text{otherwise} \tag{6.6}$$

where

$$\Delta d = \frac{\dot{u}}{PRF}$$

and

$$d_c = \frac{D}{2 \sin\alpha} \quad .$$

Then given the PRF and aperture width, the pulse-to-pulse correlation for clutter at some point on the ground beneath the aircraft may be calculated on the basis of the antenna azimuth angle to that point and the aircraft velocity. For many applications, this approximation is sufficient, and it allows a very simple calculation of pulse-to-pulse correlation. It is interesting to note that the approximation 6.6 is independent of frequency.

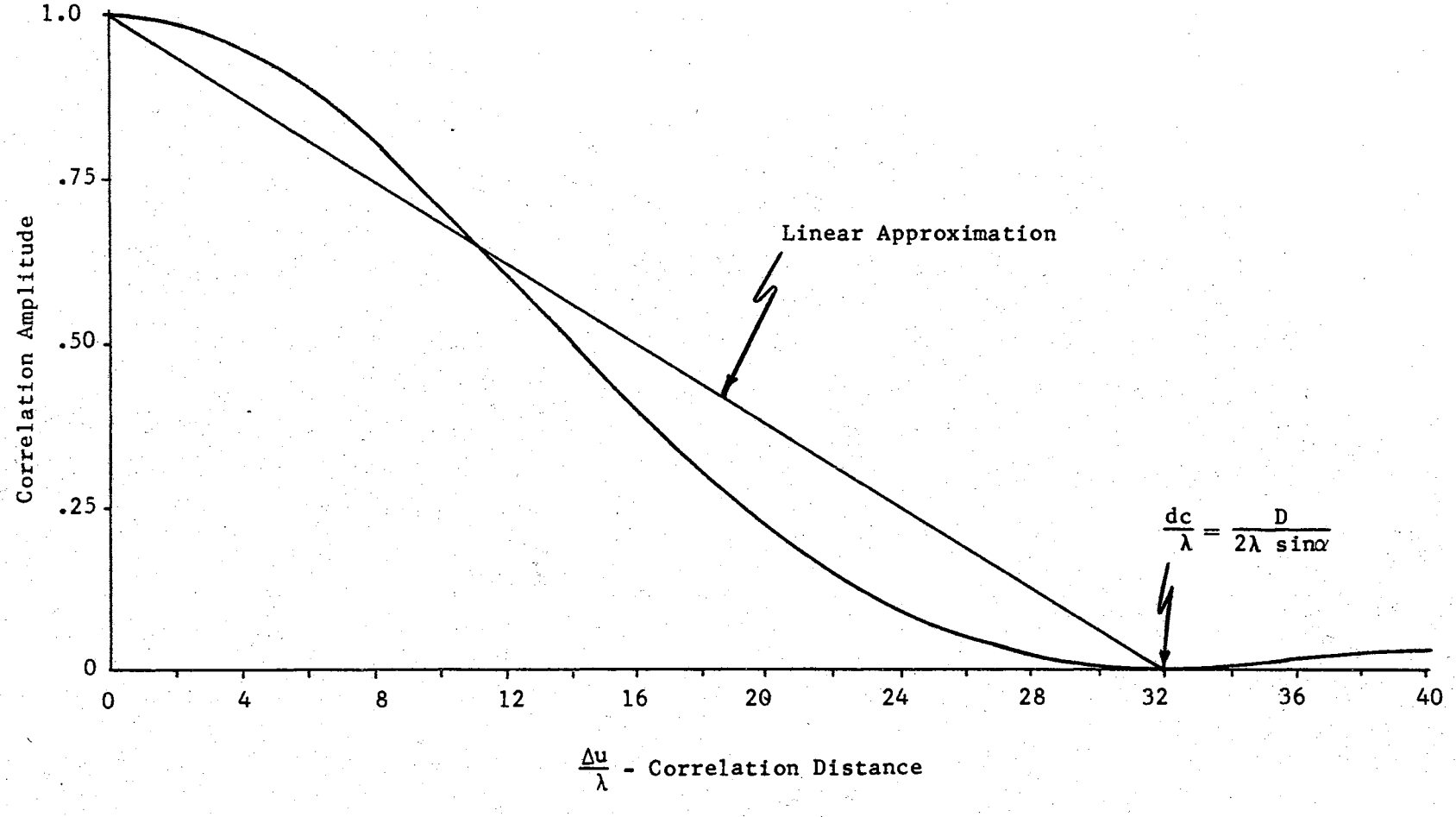

Figure 13. Linear Approximation to Autocorrelation Function

Analysis of Clutter Process Sampling

On the basis of the concept of decorrelation distance developed in this chapter, it can be shown that the aircraft must move a distance of d_c (decorrelation distance) between pulses to obtain uncorrelated pulses. Since d_c has been shown to be a function of azimuth angle, it follows that a longer time interval (or slower sampling rate) must be provided between samples of the ground taken in front of the aircraft than between samples taken to the side if the information per sample is to be kept constant. In other words, the clutter information rate is inherently higher broadside than it is ahead of the aircraft. Of course, the analysis of the clutter is a means to an end, the actual objective is to reproduce the average RCS which is being modulated by clutter. The rate at which the process should be sampled for uncorrelated samples can be shown to be

$$PRF \geq \frac{\dot{u}}{d_c} \tag{6.7}$$

where PRF is pulse repetition frequency. If RCS is sampled at a rate faster than the rate specified in relationship 6.7, then the radar will reflect a portion of the clutter variation, as well as the average RCS; this reaction is undesirable.

At this point it can be shown that the upper limits on sampling rates specified in the inequality 6.7 and the lower limits specified in the sampling theorem are each useful tools in establishing requirements for sampling. In other words, contrary to the sampling theorem, it is desirable in the present study to eliminate the variations in the process being sampled. If this reasoning is applied to the clutter

process in the frequency domain and the process were to be reproduced, the sampling rate, according to the sampling theorem, would necessarily be

$$PRF \geq 2\ BW \tag{6.8}$$

where BW is clutter bandwidth. This inequality sets a lower bound on the PRF. However to ensure that the process is not reproduced, an upper bound must be set on the PRF. It is stated in the sampling theorem that, in order to reproduce a process, samples must be taken at such a rate as to prevent aliasing, as shown by Downing (12, pages 140 to 143). However, to ensure nonreproduction of the process, a substantial degree of aliasing is necessary. In fact, it is desirable, as indicated in Figure 14 to obtain enough aliasing to produce a flat spectrum (an approximation of white noise) which may then be readily smoothed by subsequent integration.

As in the case of the sampling theorem, the sampling rate (for decorrelation in this case) is a function of process bandwidth. This can be shown by comparing the normalized spectrum bandwidths, shown in Figures 10 and 12 with the PRF derived by using decorrelation distance. The bandwidth obtained from the normalized spectra plots is a direct function of velocity in wavelengths, $\dot{u}/\lambda$, i.e., if $\dot{u}$ is doubled, the frequency scale represents a frequency twice as large. Therefore,

$$BW = K_3 \frac{\dot{u}}{\lambda} \tag{6.9}$$

where K_3 is a constant. But the sampling rate for decorrelation is

$$PRF \leq \frac{\dot{u}}{d_c} \quad ,$$

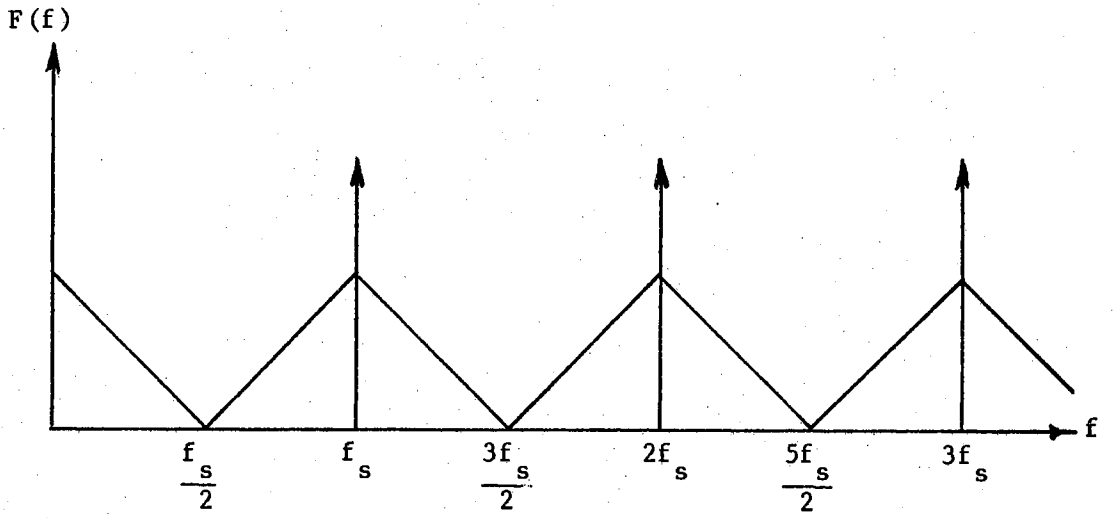

f_s = Sampling Frequency

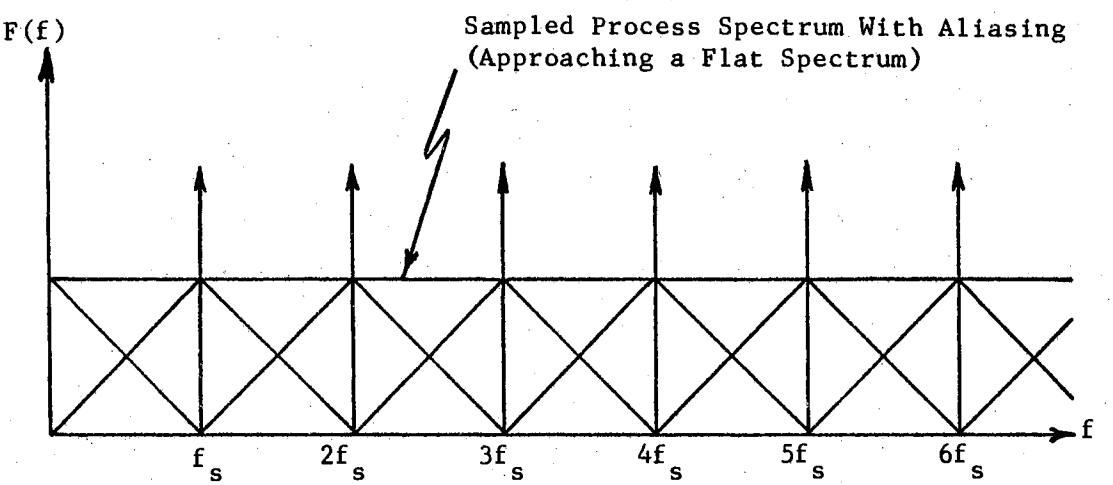

Figure 14. Results of Aliasing

and

$$d_c = \frac{57.3\ \lambda}{2\varphi\ \sin\alpha} \quad .$$

Consequently, the sampling rate for decorrelation may be written as

$$PRF \leq \frac{(BW)(2\varphi\ \sin\alpha)}{57.3\ K_3} \tag{6.10}$$

or for a given beamwidth and a given azimuth angle

$$PRF \leq (K_4)(BW) \quad . \tag{6.11}$$

If normalized frequency and normalized correlation distance as plotted in Figures 8 through 12 are designated as f_1 and t_1 respectively then

$$f_1 = \frac{f}{\dot{u}/\lambda} \tag{6.12}$$

and

$$t_1 = \frac{\Delta u}{\lambda} \quad . \tag{6.13}$$

Let f_1' and t_1' be the points where f_1 and t_1 first reach zero on the graphs. Then expressing PRF in terms of velocity and distance traveled between pulses (for decorrelation) allows

$$\frac{\dot{u}}{d_c} \leq (K_4)(BW) \tag{6.14}$$

so using Equation 6.12

$$\frac{\dot{u}/\lambda}{\frac{d_c}{\lambda}} = \frac{\dot{u}/\lambda}{t_1'} \leq (K_4)(BW) \quad . \tag{6.15}$$

The distance to the point where the previously plotted spectra reach zero in amplitude is normalized bandwidth which must be multiplied by $\dot{u}/\lambda$ to get bandwidth and expression 6.15 becomes

$$\frac{\dot{u}/\lambda}{t_1'} \leq (K_4)(\frac{\dot{u}}{\lambda})f_1' \quad . \tag{6.16}$$

Then K_4 is seen to be

$$K_4 = \frac{1}{t_1' f_1'} \quad . \tag{6.17}$$

An examination of the graphs reveals that $t_1' f_1'$ is invariant and that

$$t_1' f_1' \cong 1 \quad . \tag{6.18}$$

Therefore

$$K_4 \cong 1 \quad . \tag{6.19}$$

Then in order to ensure that uncorrelated samples are obtained, the upper bound on sampling rate can be approximated from expression 6.11 as

$$PRF \leq BW \tag{6.20}$$

which is a substantiation of the result indicated in the aliasing plots in Figure 14.

Inequality 6.20 might be considered a counter sampling theorem for clutter since it designates a sampling rate sufficient to ensure non-reproduction of the process time function.

CHAPTER VII

CLUTTER MODEL APPLICATIONS

The design of any clutter model must be based upon the applications intended for the model. In this thesis, the primary objective for the development of the model is the application of the model to clutter discrimination schemes. Therefore, the clutter model has been developed as a state model for ease of application to a recursive filtering scheme. Although the clutter process is nonstationary, a Kalman or Bayesian filtering approach is readily applicable. The nonstationarity of the process tends to make other filtering principles less applicable. However, in the application of the recursive filters developed in this chapter, it must be remembered that the process is developed on the basis of RCS, not voltage, consequently, voltage measurements must be squared before application unless they are the output of a square law detector.

Clutter discrimination schemes based upon pulse-to-pulse decorrelation and subsequent integration of the resulting noise may also be applied through use of the clutter relationships previously developed from analysis of the clutter model.

Pulse-to-Pulse Decorrelation

Some form of integration is used in most pulsed radars to smooth uncorrelated (white) noise. As shown in Chapter IV, this integration

becomes less effective in smoothing clutter as pulse-to-pulse correlation increases. Therefore, if pulse-to-pulse decorrelation can be maintained, a special clutter filter is unnecessary. The conditions necessary for pulse-to-pulse decorrelation may be determined from the expression for decorrelation distance developed in Chapter VI, which is

$$d_c = \frac{D}{2 \sin\alpha} \quad . \tag{7.1}$$

This equation indicates that, if the aircraft travels this distance (d_c) between pulses, the clutter RCS will be decorrelated. One way of obtaining this decorrelation is to vary PRF as a function of velocity and azimuth angle. A variable PRF that provides the decorrelation and simultaneously maintains a maximum clutter information rate may be obtained from Equation 6.15 as

$$(PRF)_{OPT} = \frac{2\dot{u}}{D} \sin\alpha \quad . \tag{7.2}$$

Of course, a PRF less than this also provides decorrelation but may not provide the desired average power. A varying PRF which provides approximately maximum information rate and pulse-to-pulse decorrelation is illustrated in Figure 15. As shown in this figure, the PRF decreases to some set minimum as the azimuth angle approaches zero degrees.

In most cases, it is desirable to maintain the number of pulses returned from a point target during one scan across the target (number of hits per scan) at a constant number. Therefore, if a variable PRF, such as that given by Equation 7.2, is used, a variable scan speed proportional to PRF is given by

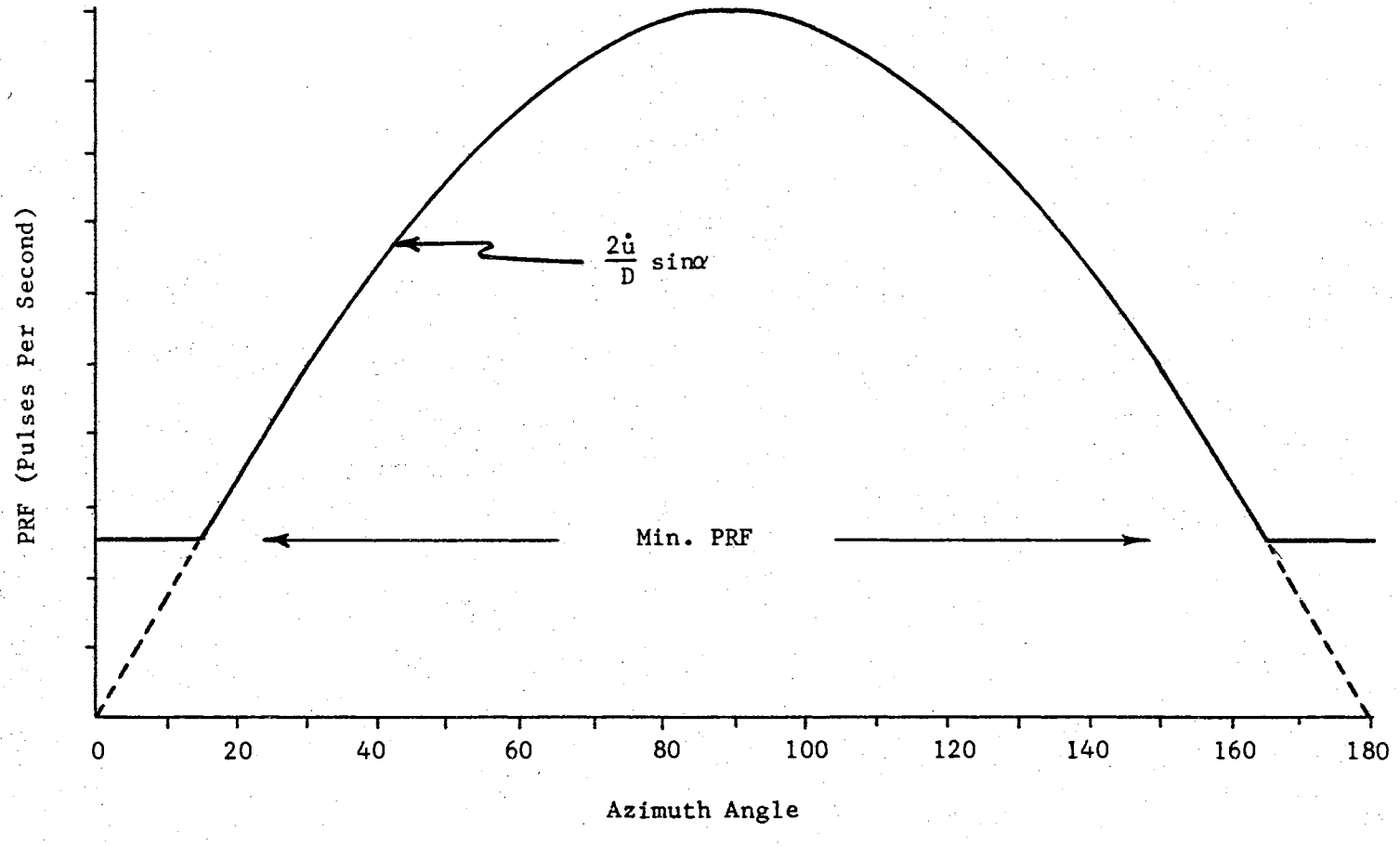

Figure 15. Variable PRF for Pulse-to-Pulse Decorrelation

$$\dot{\alpha} = \frac{(\varphi)(PRF)}{h_s} \tag{7.3}$$

is required where h_s is the symbol for hits per scan.

Scan-to-Scan Filtering

Cell RCS, σ, is a random variable which describes the fluctuation in the radar cross section of a particular clutter cell on the ground. When the same cell is tracked on a scan-to-scan basis, the radar provides discrete time (or position) measurement of the cell RCS which then fluctuates as a function of time. The value desired from a clutter filter is the mean value of cell RCS, i.e., the non-time-varying component since this mean value represents a smoothed but realistic representation of the terrain.

If M is considered a scan-to-scan index, as in Chapter IV, and if $E[\sigma_M] = X_M$ and $\sigma_M = Y_M$, then a state model of the process is

$$X_M = X_{M-1} \tag{7.4}$$

$$Y_M = X_M + \epsilon_M \quad .$$

The variance of Y_M is

$$P^2 = Var[Y_M] = \frac{N^2\sigma_i^2}{n^2}\left[n + 2\sum_{k=1}^{n-1}(n-k)r_k(k)\right] \tag{7.5}$$

where n is the number of hits per scan. The Bayesian approach can then be applied to obtain a one-dimensional Kalman filter as shown by Breipohl (14)

$$\mu_M = \frac{\mu_{M-1}P^2 + y_M S^2_{M-1}}{P^2 + S^2_{M-1}} \tag{7.6}$$

$$S^2_M = \frac{P^2 S^2_{M-1}}{P^2 + S^2_{M-1}} \tag{7.7}$$

where μ_M is the best linear estimate of X at time M and S^2_M is the variance of this estimate. Note that, as correlation increases, P^2 increases, and previous estimates are weighted more heavily, or the measured value is discounted as a result of correlation. In essence, this is a type of past-present comparison and weighting which is intuitively appealing.

If μ_0 and S^2_0 are the original values of μ_M and S^2_M, then Equations 7.6 and 7.7 may be expressed as

$$\mu_M = \frac{\mu_0 P^2 + S^2_0 \sum_{i=1}^{M} y_M}{P^2 + MS^2_0} \tag{7.8}$$

$$S^2_M = \frac{P^2 S^2_0}{P^2 + MS^2_0} \quad . \tag{7.9}$$

Then the initial values may be chosen as

$$\mu_0 = N\sigma_i \tag{7.10}$$

$$S^2_0 = N^2\sigma^2_i \tag{7.11}$$

which are simply the mean and variance of the cell RCS. These values might be obtained through measurement with the antenna pointed broadside

where correlation is minimum. Through use of these values in Equations 7.8 and 7.9 in conjunction with Equation 7.5,

$$\mu_M = \frac{\frac{N\sigma_i}{n^2}\left[n + 2\sum_{k=1}^{n-1}(n-k)r_k(k)\right] + \sum_{i=1}^{M} y_M}{\frac{1}{n^2}\left[n + 2\sum_{k=1}^{n-1}(n-k)r_k(k)\right] + M} \tag{7.12}$$

$$S_M^2 = \frac{\frac{N^2\sigma_i^2}{n^2}\left[n + 2\sum_{k=1}^{n-1}(n-k)r_k(k)\right]}{\frac{1}{n^2}\left[n + 2\sum_{k=1}^{n-1}(n-k)r_k(k)\right] + M} \quad . \tag{7.13}$$

It can be seen that $N^2\sigma_i^2$ can be divided out of Equation 7.12 so that the equation depends upon N only through the original estimate, μ_0. As shown by Breipohl (14), μ_M depends only slightly upon μ_0 after a few iterations, i.e., μ_M tends to become independent of N. Thus the filter is more or less independent of range and of terrain. However, S_M^2 is a function of N^2 and since N is a constant times slant range as shown in Appendix B, the variance of the estimate increases as a function of range squared, as does the variance of cell RCS.

The filtering process may be initiated by obtaining a measurement of average cell RCS and variance with the antenna pointing broadside (where correlation is minimum). Under these conditions, a short time-average should provide a reasonable estimate.

It has been noted in Chapter IV that scan-to-scan integration tends to degrade the time resolution of the radar, i.e., if there is change in the average cell RCS, several scans may be required to detect it. However, the filter indicated by Equation 7.6 tends to minimize this

degradation of resolution because the estimate is largely dependent on the measured value y_M when correlation is low. This filtering action is analogous to minimizing integration time (which increases response) when correlation is minimum. Thus the filter is more advantageous than straight integration which would smooth the clutter but would degrade time resolution uniformly whether integration was required to smooth clutter or not.

Pulse-to-Pulse Filtering

The Bayesian approach to Kalman filtering may also be applied on a pulse-to-pulse basis to smooth clutter. Normal distributions may be assumed since only first and second moments are known, and the use of these distributions results in an optimum linear filter as shown by Meditch (15, page 166). This is essentially the approach used by Breipohl (14), however in the present case the measurement sequence is correlated.

The state model used for this filtering is described by Equations 4.26 and 4.27 with $E[\sigma_m]$ replaced by X_m and σ_m replaced by Y_m. The state model then is

$$X_m = X_{m-1}$$

$$Y_m = X_m + \epsilon_m \quad . \tag{7.14}$$

So X_m does not vary (or varies slowly) with time and ϵ_m represents a correlated noise. The measurement variance at each instant of time is $N^2\sigma_i^2$ and will be designated here as P^2. As previously stated, the measurement sequence is assumed to be Markov-1.

Therefore in terms of normal distributions, the best mean square estimate of X, given all past values of Y_i, is the mean value of the conditional density function $f_{X|Y_n,Y_{n-1},\ldots,Y_1}$ which is normal. This conditional density function may be written in terms of known and measurable values as

$$f_{X|Y_n,Y_{n-1},\ldots,Y_1} = \frac{f_{X,Y_n|Y_{n-1},\ldots,Y_1}}{f_{Y_n|Y_{n-1},\ldots,Y_1}} = \frac{f_{Y_n|Y_{n-1},\ldots,Y_1,X} f_{X|Y_{n-1},\ldots,Y_1}}{f_{Y_n|Y_{n-1},\ldots,Y_1}}.$$

Then using the Markov-1 property

$$f_{X|Y_n,Y_{n-1},\ldots,Y_1} = \frac{f_{Y_n|Y_{n-1},X} f_{X|Y_{n-1},\ldots,Y_1}}{f_{Y_n|Y_{n-1}}} \quad . \quad (7.15)$$

It may be noted that $f_{X|Y_{n-1},\ldots,Y_1}$ is simply the conditional density function used to obtain the previous estimate and $f_{Y_n|Y_{n-1},X}$ is the conditional density function of Y_n given Y_{n-1} with a mean value X and correlation coefficient r_n. The mean and variance of Y_i are considered constants from pulse to pulse as shown in Appendix A. So the following normal density functions result:

$$f_{X|Y_{n-1},\ldots,Y_1} \sim N(\mu_{n-1}, S^2_{n-1}) \quad (7.16)$$

$$f_{Y_n|Y_{n-1},X} \sim N[x(1-r_n) + r_n y_{n-1}, P^2(1-r_n)] \quad (7.17)$$

where

μ_{n-1} is the previous estimate

S^2_{n-1} is the variance of the previous estimate.

These two normal density functions may be combined in Equation 7.15 to obtain a new normal density function. The mean and variance of this new density function then describe the present estimate and its variance. These may be obtained as

$$\mu_n = \frac{S_{n-1}^2(y_n - r_n y_{n-1}) + \mu_{n-1}P^2(1+r_n)}{S_{n-1}^2(1-r_n) + P^2(1+r_n)} \tag{7.18}$$

$$S_n^2 = \frac{S_{n-1}^2 P^2(1+r_n)}{S_{n-1}^2(1-r_n) + P^2(1+r_n)} \quad . \tag{7.19}$$

An inspection of Equation 7.18 will reveal that as pulse-to-pulse correlation increases, the previous estimate is weighted more heavily and the present measurement is discounted by subracting from it the information common to the previous measurement. If correlation is zero ($r_n = 0$) the equations become the simple one-dimensional Kalman filter equations for uncorrelated measurement noise. Therefore Equation 7.18 might be considered an optimum weighting between the previous estimate and the new information (uncorrelated portion) available in the current measurement. The previous estimate is weighted by the autocorrelation function of the measurement and the new information is weighted by the variance of the previous estimate.

Equations 7.18 and 7.19 may be expressed in terms of the initial values as

$$\mu_n = \frac{S_0^2\left[\sum_{j=1}^{n}(y_j - r_n y_{j-1})\right] + \mu_0 P^2(1+r_n)}{nS_0^2(1-r_n) + P^2(1+r_n)} \tag{7.20}$$

$$S_n^2 = \frac{S_0^2 P^2 (1+r_n)}{nS_0^2(1-r_n) + P^2(1+r_n)} \tag{7.21}$$

where

$j = 1,2,\ldots,n$

$y_0 = 0.$

Again, as in the scan-to-scan case, if μ_0 and S_0^2 are taken as $N\sigma_i$ and $N^2\sigma_i^2$, respectively, then μ_n tends to become independent of terrain and S_n^2 increases with increased slant range. These initiating estimates may be measured as in the scan-to-scan case by pointing the antenna broadside where clutter correlation is minimum, and measuring the time average and variation about this average.

Comparison of Filtering Schemes

Since two different approaches to recursive clutter filtering have been presented, it seems appropriate to discuss the relative merits of the two. In each case, even though use is made of recursive filtering which involves storing only one past value, considerable computer storage is still required, if a large section of ground return is to be smoothed, since the filter equations must be applied independently to each resolution cell. However, in the scan-to-scan case where approximately n pulses are integrated (n hits per scan) prior to clutter smoothing, a saving of computer storage of up to 1/n might be realized, depending upon how the correlation information is implemented.

Although pulse-to-pulse filtering involves more computer storage and more complexity, it offers the possibility of avoiding the time

resolution degradation inherent in scan-to-scan filtering. The usual integration resulting from post-detection filtering and CRT smoothing tends to destroy any time resolution on a pulse-to-pulse basis; consequently, any recursive pulse-to-pulse smoothing prior to post-detection filtering and CRT smoothing should have little effect upon the time resolution. Pulse-to-pulse filtering involves a reinitiation of the filtering process with the start of each new scan since the last pulse of a previous scan is generally uncorrelated with the first pulse of a present scan. The process could be initiated at the beginning of each scan by using the averaged value from the previous scan as an initial estimate of cell RCS; however, the filtering action depends upon pulse-to-pulse correlation; therefore, two measurements must be made before pulse-to-pulse correlation can be applied correctly and before the correct filtering can begin.

Comparison of Clutter Decorrelation Schemes

Pulse-to-pulse clutter decorrelation is obtained by causing a substantial pulse-to-pulse change in phase difference between the returns from the elementary scatterers within a clutter cell. This change can be effected by translating the radar position between pulses by a sufficient amount to alter the relative distances between scatterers since this alteration will change the phase difference. This can also be accomplished by varying the number of wavelengths (which is phase) between scatterers. Changing the number of wavelengths between scatterers may be accomplished by changing the length of a wave. Consequently, decorrelation may be accomplished by changing frequency on a pulse-to-pulse basis.

O'Leary (6, pages 6 through 11) showed the frequency change necessary to decorrelate the return from a target of given size. This decorrelation effect and the clutter smoothing resulting from frequency jumping were also reported by Gustafson (7). By using sea clutter, Croney (5) demonstrated that, if sufficient time is allowed between pulses for pulse-to-pulse decorrelation, clutter smoothing results from subsequent integration. Thus any scheme which produces pulse-to-pulse decorrelation is effective but each places some limitation on the radar. To obtain an efficient use of the concept of waiting one decorrelation time between pulses, it is necessary to be able to determine decorrelation time. The model developed in this thesis provides a realistic estimate of this decorrelation time.

It appears that, although the filtering presented in this chapter reduces ground clutter, it is suboptimal in that energy or average power is used to gather correlated samples which must then be filtered. Since less energy is required, a more efficient scheme is to gather the same information by using fewer uncorrelated samples (at the maximum rate of availability of the information, if desired). The uncorrelated noise may then be smoothed through integration.

CHAPTER VIII

SUMMARY AND CONCLUSIONS

This thesis has been directed to developing a mathematical model for airborne radar ground clutter which may be applied in clutter discrimination schemes.

Summary

The clutter model is developed by first assuming that terrain is characterized by several rather general characteristics which have also been assumed in most previous studies of a similar nature. From these assumptions, a probability density function is developed to describe the separation of elementary scatterers within a resolution cell. This density function represents the basic randomness assumed; consequently, it is called the statistical model. The geometry of the aircraft motion and cell position are developed in a deterministic model which relates the statistical model to aircraft motion. A phasor addition of the radar cross section of the elementary scatterers is then used to relate the deterministic and statistical models to cell radar cross section. Time is introduced by examining radar cross section from the standpoint of discrete state model results which are obtained on the basis of a pulse-to-pulse comparison. Evaluation of the moments of the resulting radar cross section random process provides a clutter autocorrelation function which is shown to be the basic clutter relationship. The

state model in conjunction with the various first and second moments, is defined as the basic mathematical model.

The autocorrelation function is analyzed by calculating its Fourier transform; this transform represents the power squared spectrum. The autocorrelation function and spectrum are plotted in three dimensions to gain insight into the process. A basic quantity called decorrelation distance is developed from the graphical analysis (the plots) and is found to be an approximate function of antenna aperture width and azimuth angle. This decorrelation distance, which is the distance the aircraft must travel between pulses to obtain decorrelated pulses, is shown to be directly related to process bandwidth since either is sufficient to describe the sampling rate necessary for decorrelation.

The completely developed clutter model is finally applied in several schemes of clutter discrimination. These schemes basically involve (1) control of radar PRF to obtain decorrelation and (2) recursive filtering to reduce the effects of correlation.

Conclusions

Analysis of the clutter model developed in this thesis indicates that ground clutter is a nonstationary random process whose spectrum varies primarily as a function of wavelength, antenna aperture width, azimuth angle, and aircraft velocity. Decorrelation distance, which is inversely related to spectrum width, is shown to be approximated by

$$d_c = \frac{D}{2 \sin\alpha}$$

where D is aperture width and α is azimuth angle. Thus ground clutter

information from a moving aircraft is available at a faster rate at angles approximately normal to the direction of motion than at angles near the direction of motion.

Several of the basic characteristics of airborne radar ground clutter have been tentatively identified in the process of building the clutter model:

(1) Clutter increases with correlation.

(2) Clutter varies inversely as the sine of azimuth angle.

(3) Correlation is invariant with range beyond some minimum range; consequently, clutter increases with range only because clutter variance increases with range.

(4) Clutter tends to become invariant with both altitude and pulse width beyond some minimum range points off ground track.

(5) Clutter decreases with increased aircraft velocity.

(6) Clutter decreases with decreased wavelength.

(7) Clutter decreases with increased antenna beamwidth.

The clutter model developed in this thesis provides a tool which may be used to gain insight into the clutter process and may be applied in clutter discrimination schemes.

Recommendations for Further Study

The mathematical model developed in this thesis is approached from the viewpoint of the clutter cell RCS rather than that of the returned voltage. An interesting extension of this study would be to start with the same assumptions and develop a voltage model which could be used to determine which approach produces a more useful model on the basis of a comparison of the two models.

Two of the assumptions made in this study are that the elementary scatterers within a cell are equal in amplitude and that the RCS randomness is introduced through scatterer separation. If the elementary scatterer amplitude were given some random distribution, the model could then incorporate an additional degree of randomness and the resulting clutter model might be more precise, but it would certainly be more complicated.

An interesting relationship between clutter bandwidth and some maximum sampling rate for pulse-to-pulse clutter decorrelation is approximated in Chapter VI. The development of a more detailed statement of this relationship might lead to a more general application in the analysis of the sampling necessary for smoothing other correlated random processes.

The clutter model developed in this study could be applied in other areas of radar technology, each of which would result in further study. The following are a few examples:

(1) Filtering by analog means.

(2) Analysis for target detection in clutter.

(3) Simulation of ground clutter.

(4) Analysis of moving target indication (MTI) in clutter.

SELECTED BIBLIOGRAPHY

(1) Rice, S. O. "Mathematical Analysis of Random Noise." Bell System Tech. J. Vol. 23 (1944), 282-332, Vol. 24 (1945), 46-156.

(2) George, T. S. "Fluctuations of Ground Clutter Return in Airborne Radar Equipment." Proc. IEE (London). Vol. 99 (April, 1952), 92-99.

(3) Urkowitz, H. "Filters for Detection of Small Signals in Clutter." J. Appl. Phys. Vol. 24 (August, 1953), 1024-1031.

(4) Rihaczek, A. W. "Optimum Filters for Signal Detection in Clutter." IEEE Trans. Aerospace Electron. Systems. Vol. AES-1 (1965), 297-299.

(5) Croney, J. "Improved Radar Visiblity of Small Targets in Sea Clutter." The Radio and Electronic Engineer. Vol. 32 (September, 1966), 135-147.

(6) O'Leary, J. J., and H. K. Ray. "Notes on Frequency Agility." General Electric Company, Syracuse, N. Y. G. E. Rpt. No. LM 37-104942. (December, 1961).

(7) Gustafson, B. G. "System Properties of Jumping-Frequency Radars." Philips Telecommunication Review (Sweden). Vol. 25 (July, 1964), 70-76.

(8) Greenstein, L. J. "A Comprehensive Ground Clutter Model for Airborne Radars." Illinois Institute of Technology, Chicago, Illinois. Air Force Contract F33615-69-C-1387. (September, 1969.

(9) Dickey, T. R. "Theory of Correlation Aircraft Navigator." General Electric Company, Syracuse, N. Y. TIS No. R 59ELS-90. (1959), 1-16.

(10) Rihaczek, A. W. Principles of High-Resolution Radar. New York: McGraw-Hill, 1969.

(11) Papoulis, Athanasios. Probability, Random Variables and Stochastic Processes. New York: McGraw-Hill, 1965.

(12) Downing, John J. Modulation Systems and Noise. Englewood Cliffs: Prentice-Hall, Inc., 1964.

(13) Costas, John P. "Periodic Sampling of Stationary Time Series." MIT Tech. Rpt. No. 156. (May, 1950).

(14) Breipohl, Arthur M. "Kalman Filtering and its Application to Reliability." IRE Transactions on Reliability. Vol. R-18 (August, 1969).

(15) Meditch, J. S. Stochastic Optimal Linear Estimation and Control. New York: McGraw-Hill, 1969.

(16) Povejsil, D. J., R. S. Raven, and Peter Waterman, eds. Airborne Radar. Princeton: D. Van Nostrand Company, Inc., 1961.

APPENDIX A

MEAN AND VARIANCE

Process mean and variance are established on the basis of the following rationale. If time is held constant and cell RCS, σ, is considered a function of N and σ_i, then N and/or σ_i might be considered random variables which could account for terrain changes. However, only the time variations are considered in this thesis; consequently, a uniform terrain distribution is assumed, and N and σ_i are constants for a given resolution cell size and a given terrain. The moments of σ under consideration in this Appendix are the aircraft motion (or time) moments evaluated at zero time change and are therefore constants.

The expected value of σ is found by considering σ in the form obtained in Equation 4.9, i.e.,

$$\sigma = N\sigma_i + 2\sigma_i \sum_{\ell=1}^{\frac{N(N-1)}{2}} \cos\Delta\theta_\ell \quad . \tag{A.1}$$

Then

$$E[\sigma] = N\sigma_i + 2\sigma_i \sum_{\ell=1}^{\frac{N(N-1)}{2}} E[\cos\Delta\theta_\ell] \quad . \tag{A.2}$$

But from Equation 3.12

$$E[\cos\Delta\theta_\ell] = E[\cos\ a\ Z_1] \quad . \tag{A.3}$$

Then using the marginal density function of Z_1 given in Chapter II

$$E[\cos\Delta\theta_\ell] = \int_{-K_1}^{K_1} (\cos az_1)[\frac{1}{K_1}(1 - \frac{|z_1|}{K_1})]dz_1 \qquad (A.4)$$

$$= \frac{\sin^2 \frac{aK_1}{2}}{(\frac{aK_1}{2})^2} \quad .$$

But

$$\frac{aK_1}{2} = (\frac{2\pi}{\lambda} \sin\gamma_2)K_1 \quad . \qquad (A.5)$$

So for

$$K_1 \gg \lambda \quad ,$$

which is valid for all conventional airborne radars, then

$$\frac{aK_1}{2} \gg 1 \qquad (A.6)$$

and

$$E[\cos\Delta\theta_\ell] \cong 0 \quad . \qquad (A.7)$$

Therefore Equation A.2 becomes approximately

$$E[\sigma] = N\sigma_i \quad . \qquad (A.8)$$

The mean squared value of σ will be found to be $2N^2\sigma_i^2$ in a similar fashion. Consider, from Equation 4.10,

$$E[\sigma^2] = E\left[N\sigma_i + 2\sigma_i \sum_{\ell=1}^{\frac{N(N-1)}{2}} \cos\Delta\theta_\ell \right]^2 \qquad (A.9)$$

$$= N^2\sigma_i^2 + 4N\sigma_i^2 \sum_{\ell=1}^{\frac{N(N-1)}{2}} E[\cos\Delta\theta_\ell] + 4\sigma_i^2 E\left[\sum_{\ell=1}^{\frac{N(N-1)}{2}} \cos\Delta\theta_\ell \right]^2 .$$

However $E[\cos\Delta\theta_\ell] = 0$, therefore it is sufficient to show the last term in the above equation is equal $N^2\sigma_i^2$. Expressing the square as a double summation

$$E\left[\sum_{\ell=1}^{\frac{N(N-1)}{2}} \cos\Delta\theta_\ell \right]^2 = E\left[\sum_{\ell=1}^{\frac{N(N-1)}{2}} \sum_{m=1}^{\frac{N(N-1)}{2}} \cos\Delta\theta_\ell \cos\Delta\theta_m \right] . \qquad (A.10)$$

But $\Delta\theta_\ell$ and $\Delta\theta_m$ are independent so

$$E[\cos\Delta\theta_\ell \cos\Delta\theta_m] = 0 \qquad \text{for } m \neq \ell \qquad (A.11)$$

$$= E[\cos^2\Delta\theta_\ell] \qquad \text{for } m = \ell \quad .$$

The double summation then reduces to a single summation and using a trigonometric identity

$$E[\cos^2\Delta\theta_\ell] = E[\tfrac{1}{2} + \frac{\cos 2\Delta\theta_\ell}{2}]$$

$$= \tfrac{1}{2} + \tfrac{1}{2} E[\cos 2\Delta\theta_\ell] \quad . \qquad (A.12)$$

But

$$E[\cos 2\Delta\theta_\ell] = E[\cos 2aZ_1] = 0 \qquad \text{(A.13)}$$

by the same argument used above for $E[\cos aZ_1]$. So

$$E\left[\sum_{\ell=1}^{\frac{N(N-1)}{2}} \cos\Delta\theta_\ell\right]^2 = E\left[\sum_{\ell=1}^{\frac{N(N-1)}{2}} \cos^2\Delta\theta_\ell\right] = \frac{N(N-1)}{2}\left(\frac{1}{2}\right) \quad .$$

Therefore from Equation A.9 it is seen that

$$E[\sigma^2] = N^2\sigma_i^2 + 4\sigma_i^2\left[\frac{N(N-1)}{2}\left(\frac{1}{2}\right)\right] \qquad \text{(A.14)}$$

$$= N^2\sigma_i^2 + N(N-1)\sigma_i^2$$

$$\cong 2N^2\sigma_i^2$$

for large N. Then the variance of σ is given by

$$\mathrm{Var}[\sigma] = E[\sigma^2] - E^2[\sigma] \qquad \text{(A.15)}$$

$$= 2N^2\sigma_i^2 - N^2\sigma_i^2$$

$$= N^2\sigma_i^2 \quad .$$

APPENDIX B

DEVELOPMENT OF VARIANCE AND AUTOCOVARIANCE FUNCTION

The variance, S_m^2, of the random variable b_m is the variance between σ_m and σ_{m-1}. However by letting the time interval between m-1 and m vary, a continuous function of time difference or distance traveled, Δu, is obtained. The time difference of interest for the radar problem is typically less than a second; consequently, over a period on the order of a second, it is assumed that the probability density function given by Equation 2.8 does not change (i.e., short-term stationarity is assumed). It can be seen from the analysis of the autocovariance function in Chapter V that, in the case of typical airborne radars, the correlation is essentially zero after a movement, Δu, of a few feet or is essentially zero after a few milliseconds at a speed of 600 miles per hour. Therefore, it is typically necessary to assume short-term stationarity over only a few milliseconds and only in the wide sense (i.e., no change in first-order and second-order moments over the time interval) since only first-order and second-order moments are used.

S_m^2 will be derived by beginning with Equation 4.17,

$$S_m^2 = 4\sigma_i^2 \, E\left[\sum_{k=1}^{\frac{N(N-1)}{2}} \cos^2\Delta\theta_{k,m} + \cos^2\Delta\theta_{k,m-1} - 2\cos\Delta\theta_{k,m}\cos\Delta\theta_{k,m-1} \right].$$

Then assuming no change in the density function from m-1 to m,

$$E[\cos^2\Delta\theta_{k,m-1}] = E[\cos^2\Delta\theta_{k,m}]$$

$$= \frac{1}{2} \tag{B.1}$$

as shown in Appendix A, and

$$S_m^2 = 4\sigma_i^2[\frac{N(N-1)}{2}(\frac{1}{2}+\frac{1}{2})] - 4\sigma_i^2 \sum_{k=1}^{\frac{N(N-1)}{2}} 2E(\cos\Delta\theta_{k,m}\cos\Delta\theta_{k,m-1})$$

$$= 2N^2\sigma_i^2 - 2N^2\sigma_i^2 r_m(u,v,\Delta u) \tag{B.2}$$

for large N. Therefore using a trigonometric identity and Equation 4.18

$$r_m = 2E[\cos\Delta\theta_{k,m}\cos\Delta\theta_{k,m-1}]$$

$$= 2E[\frac{1}{2}\cos\delta_m + \frac{1}{2}\cos(2\Delta\theta_{k,m-1} + \delta_m)] \tag{B.3}$$

$$= E[\cos\delta_m] + E[\cos(2\Delta\theta_{k,m-1} + \delta_m)]$$

as shown in Equation 4.18 where $\delta_m = (\Delta\theta_{k,m} - \Delta\theta_{k,m-1}) = (d_1Z_1+d_2Z_2)\Delta u$. The second term in Equation B.3 may be seen to be approximately zero by the same argument used in Appendix A. Therefore

$$r_m = E[\cos\delta_m] \quad . \tag{B.4}$$

Evaluation of r_m requires multiplication of $\cos\delta_m$ times the density function developed in Chapter II and integration. So using Equations 3.13 and 4.18

$$E[\cos\delta_m] = \int_{-K_2}^{K_2} \int_{-K_1}^{K_1} \cos[(d_1 z_1 + d_2 z_2)\Delta u] f_{Z_1,Z_2}(z_1,z_2)\,dz_1\,dz_2 \quad (B.5)$$

which must be divided into four integrals, one for each quadrant of the density function, for integration. In the first quadrant only the integral is

$$E[\cos\delta_m]_1 = \frac{1}{K_1 K_2} \int_0^{K_2} \int_0^{K_1} \cos[(d_1 z_1 + d_2 z_2)\Delta u](1 - \frac{z_1}{K_1})(1 - \frac{z_2}{K_2})\,dz_1\,dz_2 \,. \quad (B.6)$$

Performing the indicated integrations results in

$$r_m(u,v,\Delta u) = \left[\frac{\sin \frac{d_1 K_1 \Delta u}{2}}{\frac{d_1 K_1 \Delta u}{2}} \; \frac{\sin \frac{d_2 K_2 \Delta u}{2}}{\frac{d_2 K_2 \Delta u}{2}} \right]^2 \quad (B.7)$$

and the autocovariance function shown in Equation 4.25 is

$$R_m(u,v,\Delta u) = N^2 \sigma_i^2 r_m(u,v,\Delta u) \quad . \quad (B.8)$$

Therefore from Equation 4.24

$$S_m^2(u,v,\Delta u) = 2N^2 \sigma_i^2 [1 - r_m(u,v,\Delta u)] \quad . \quad (B.9)$$

Since r_m is a function of position and change in position and thus a function of time, the process is obviously nonstationary in general.

The value N which is the number of elementary scatterers within a resolution cell has been assumed to be constant up to this point. Since

the number of scatterers within a cell is a direct function of cell area, N is essentially constant on a pulse-to-pulse or scan-to-scan basis (i.e., N is slowly varying). However N is actually a function of the slant range (r) to the cell since for a given terrain type the number of scatterers within a cell depends upon cell area. Cell area is given by

$$K_1 K_2 = [\frac{c\tau}{2} \csc \gamma_2][r\varphi] \tag{B.10}$$

and it can be seen that cell area is a direct function of r. So N can be expressed as

$$N = K_a r$$

where K_a is constant for a fixed pulse width, fixed beamwidth and at ranges larger than altitude.

The value N then is considered deterministic; therefore treating it as a constant in the analysis of expected values causes no error. In fact N does not appear in the normalized autocovariance function developed in this Appendix, instead it appears in the mean and variance of σ as shown in Equations A.8 and A.15. Therefore cell RCS mean and variance both increase with slant range, but they are approximately constant from pulse to pulse and scan to scan.

The value of radar cross section of the individual scatterers within a cell, σ_i, is considered constant although obviously as the ground reflection coefficient, σ_0, changes, σ_i changes. However, for a given terrain type σ_0 is shown to be relatively constant over a wide range of grazing angles (8). Thus only at very short or very long ranges will the assumption of σ_i constant with range cause serious error.

APPENDIX C

COMPARISON OF POWER AUTOCOVARIANCE WITH VOLTAGE AUTOCOVARIANCE

RCS clutter is proportional to clutter voltage squared; therefore the Fourier transform of RCS clutter autocovariance (or autocorrelation since the process has zero mean) provides a spectrum analogous to the power squared spectrum while the Fourier transform of clutter voltage autocovariance provides the conventional power spectrum. Both autocovariance functions provide essentially the same information although in different forms. The mathematics involved in finding the voltage autocovariance function become very involved, and most investigations end up by imposing limitations in order to obtain approximations of the function. As pointed out by Raven (16, page 262) in referring to this problem in general,

> Instead of becoming involved with such approximations, however, it is often either more convenient analytically or more realistic in a physical sense to assume that the second detector is a square law rectifier producing the square of the envelope rather than the envelope itself.

Raven (16, pages 245 to 264) discusses this general problem of the power density spectrum at the output of nonlinear devices; this problem is closely related to the particular problem considered in this Appendix.

Since the RCS clutter is specified in terms of a voltage squared in the time domain, descriptions of RCS clutter autocovariance will generally take the form of a function of the square of the clutter voltage autocovariance. Since squaring in the time domain implies

self-convolution in the frequency domain, a spectral comparison of the two functions indicates the RCS clutter spectrum (power squared) should tend to be wider than the conventional power spectrum.

To obtain an approximate comparison of the RCS autocovariance function generated in this thesis with the analogous voltage function, assume that the voltage components of clutter at time 1 and 2 given here by X_1 and X_2 are jointly normal with zero mean and correlation coefficient ρ (which could be argued as a good approximation). Then the voltage autocovariance is given by Raven (16) as

$$E[X_1X_2] = \frac{1}{2\pi\sigma^2\sqrt{1-\rho^2}} \int_{-\infty}^{\infty} \int_{-\infty}^{\infty} x_1x_2 \exp\left[\frac{-x_1^2 + 2\rho x_1x_2 - x_2^2}{2\sigma^2(1-\rho^2)}\right]dx_1dx_2$$

$$= \sigma^2\rho(\tau) \qquad (C.1)$$

with $E[X^2] = \sigma^2$. Then if the voltage squared is considered, i.e.,

$$y = x^2 \qquad (C.2)$$

the following results may be obtained,

$$E[Y] = \sigma^2 \qquad (C.3)$$

$$E[Y^2] = 3\sigma^4 \qquad (C.4)$$

$$\sigma_y^2 = 2\sigma^4 \quad . \qquad (C.5)$$

The autocorrelation function of Y given by Raven (16, page 254) is

$$E[Y(t)Y(t+\tau)] = \frac{1}{2\pi\sqrt{1-\rho^2\sigma^2}} \int_{-\infty}^{\infty}\int_{-\infty}^{\infty} x_1^2 x_2^2 \exp\left[\frac{-x_1^2+2\rho x_1 x_2 - x_2^2}{2\sigma^2(1-\rho^2)}\right] dx_1 dx_2$$

$$= \sigma^4(1 + 2\rho^2(\tau)) \quad . \tag{C.6}$$

The normalized autocovariance function then for the voltage squared is $\rho^2(\tau)$, which in this case is the square of the normalized voltage autocovariance. If it is now assumed that a similar relationship holds for the autocovariance function developed in Appendix B then an approximation of the normalized voltage autocovariance is simply $(r_m)^{\frac{1}{2}}$ where r_m is given in Equation 5.1. A plot of this approximation compared with the clutter RCS autocovariance is shown in Figure 16. This approximation to the voltage autocovariance given by $(r_m)^{\frac{1}{2}}$ is seen to be somewhat broader than r_m and this will result in a narrowing of the spectrum as predicted. However the decorrelation distance defined as the distance to the first zero crossing remains unchanged. Figure 16 also shows that the square root of the linear approximation of r_m is a close approximation to this function obtained for the voltage autocovariance. Therefore a reasonable approximation to the clutter voltage normalized autocovariance function appears to be (using Equation 6.14)

$$\psi_m = \left[1 - \frac{\Delta d}{d_c}\right]^{\frac{1}{2}} \tag{C.7}$$

$$= \left[\frac{.5D/\sin\alpha - \frac{\dot{u}}{PRF}}{.5D/\sin\alpha}\right]^{\frac{1}{2}} \qquad \text{for } \Delta d < d_c$$

$$= 0 \qquad \text{elsewhere} \quad .$$

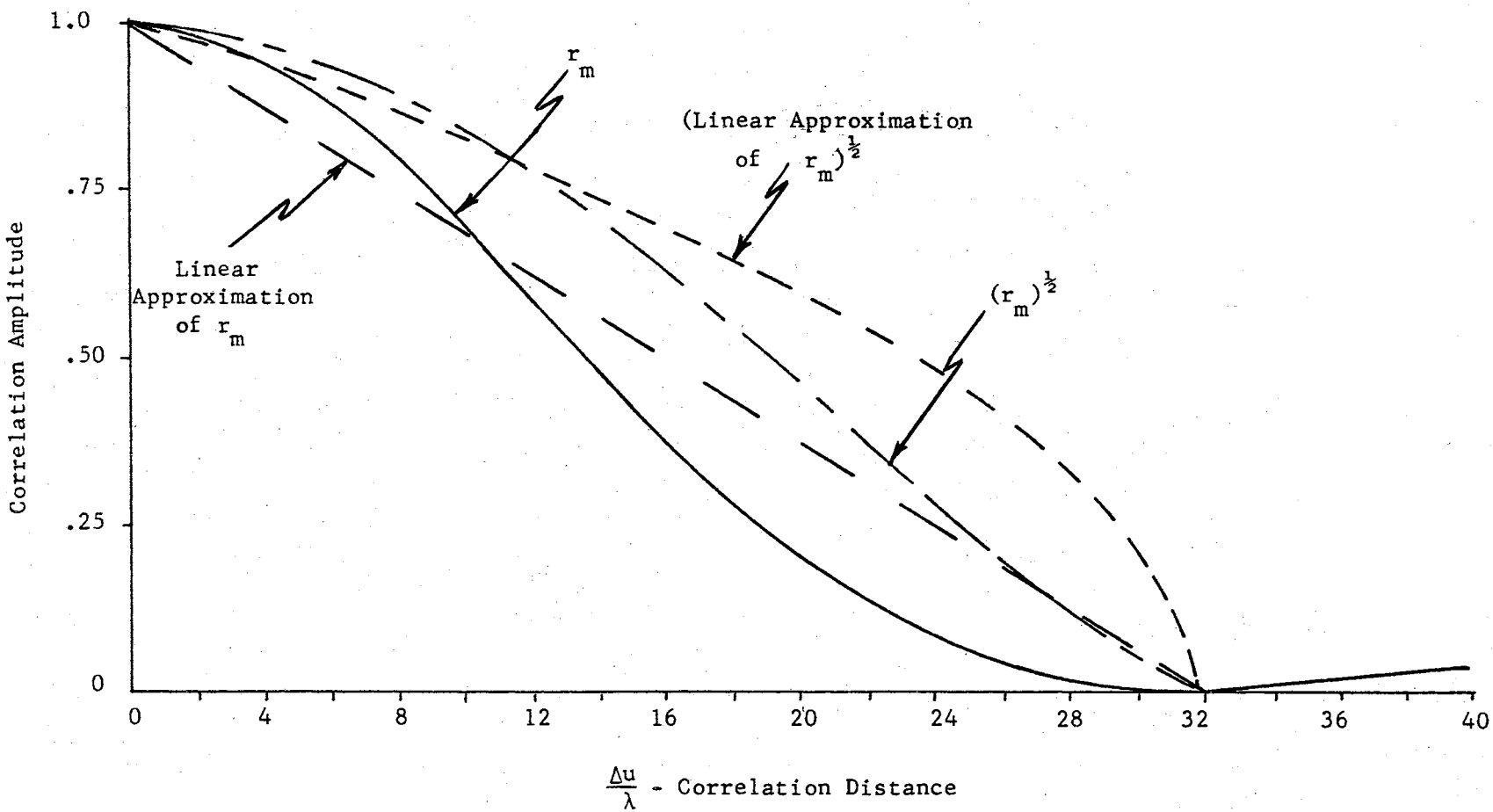

Figure 16. Approximation Comparisons

A calculation of the clutter voltage autocovariance function in a more general fashion for comparison with the RCS autocovariance function appears to be a formidable task and will not be undertaken. It is not clear which form of the clutter autocovariance function is more basic but either form will allow some insight into the complicated process.

APPENDIX D

NORMALIZED FOURIER TRANSFORM OF AUTOCOVARIANCE

The autocovariance function of the RCS process may be assumed to be short-term stationary which is discussed in Appendix B. Then, in accordance with the Wiener-Kinchine relation discussed by Downing (12, page 37), the Fourier transform pair

$$G(\omega) = \int_{-\infty}^{\infty} r(t)e^{-j\omega t}dt \tag{D.1}$$

$$r(t) = \int_{-\infty}^{\infty} G(\omega)e^{j\omega t}df \tag{D.2}$$

represent the normalized autocovariance function and its power spectral density. However, since r(t) in this case is analogous to a voltage-squared relationship, a power-squared spectral density results.

For notational convenience, the following set of relations are defined, some in terms of previously designated constants (d_1, d_2, K_1, K_2 are designated in Chapter III):

f = frequency in hertz

$\omega = 2\pi f$

$t = \frac{\Delta u}{\dot{u}}$

$\alpha = \frac{d_1 K_1 \Delta u}{2t} = \frac{d_1 K_1 \dot{u}}{2}$

$$\beta = \frac{d_2 K_2 \Delta u}{2t} = \frac{d_2 K_2 \dot{u}}{2}$$

$$\alpha_1 = \frac{uh^2 c\tau}{2r^2(u^2+v^2)}$$

$$\beta_1 = \frac{\varphi v}{\sqrt{u^2+v^2}} \quad .$$

Thus the autocovariance function given in Equation 5.1 may be written as

$$r(t) = \left[\frac{\sin\alpha t}{\alpha t} \quad \frac{\sin\beta t}{\beta t}\right]^2 \quad . \tag{D.3}$$

Then the Fourier transform of r(t) is

$$G(\omega) = \int_{-\infty}^{\infty} r(t)[\cos\omega t - j \sin\omega t]dt \quad . \tag{D.4}$$

But r(t) is an even function so r(t)sinωt is odd and the integral of an odd function over symmetrical limits is zero. Therefore

$$G(\omega) = \int_{-\infty}^{\infty} \left[\frac{\sin\alpha t \sin\beta t}{\alpha\beta t^2}\right]^2 \cos\omega t dt \quad . \tag{D.5}$$

By using trigonometric identities to expand this integral, it may be broken into nine integrals of the form

$$\int_{-\infty}^{\infty} \frac{\cos\omega t}{t^4} dt = \frac{\omega^3}{6} (4\pi) \tag{D.6}$$

and

$$G(\omega) = \frac{\pi}{12(\alpha\beta)^2}\{2\omega^3-(\omega+2\alpha)^3-|\omega-2\alpha|^3-(\omega+2\beta)^3-|\omega-2\beta|^3+\tfrac{1}{2}[\omega+(\alpha+\beta)]^3$$

$$+\tfrac{1}{2}|\omega-(\alpha+\beta)|^3+\tfrac{1}{2}|\omega+(\alpha-\beta)|^3+\tfrac{1}{2}|\omega-(\alpha-\beta)|^3\} \quad . \tag{D.7}$$

This function is then normalized in terms of wavelength and velocity by performing a scale change given by

$$F(f) = \frac{1}{2\pi|J|}\,G\left(\frac{\omega}{2\pi J}\right) \tag{D.8}$$

where J is a constant to be designated. Since

$$\frac{\Delta u}{\lambda} = \frac{\dot{u}t}{\lambda} \tag{D.9}$$

where t is the time to travel a distance Δu,

$$J = \frac{\dot{u}}{\lambda} \tag{D.10}$$

and

$$F(f) = \frac{1}{2\pi\frac{\dot{u}}{\lambda}}\,G\left(\frac{\omega}{2\pi\frac{\dot{u}}{\lambda}}\right) \tag{D.11}$$

$$= \frac{\lambda}{2\pi\dot{u}}\,G\left(\frac{f}{\frac{\dot{u}}{\lambda}}\right) \quad .$$

Then $\dfrac{f}{\frac{\dot{u}}{\lambda}}$ is seen to be dimensionless so let

$$f_1 = \frac{f}{\frac{\dot{u}}{\lambda}} \tag{D.12}$$

and

$$\frac{\dot{u}}{\lambda} F(f_1) = \frac{1}{2\pi} G(f_1) \quad . \tag{D.13}$$

Then since α and β may be expressed as

$$\alpha = \frac{2\pi \dot{u} \alpha_1}{\lambda} \tag{D.14}$$

and

$$\beta = \frac{2\pi \dot{u} \beta_1}{\lambda} \quad , \tag{D.15}$$

these may be substituted into Equation D.7. This substitution and the indicated scale change results in

$$\frac{\dot{u}}{\lambda} F(f_1) = \frac{1}{24(\alpha_1\beta_1)^2} \{2f_1^3 - (f_1+2\alpha_1)^3 - |f_1-2\alpha_1|^3 - (f_1+2\beta_1)^3 - |f_1-2\beta_1|^3$$

$$+ \tfrac{1}{2}[f_1+(\alpha_1+\beta_1)]^3 + \tfrac{1}{2}|f_1-(\alpha_1+\beta_1)|^3 + \tfrac{1}{2}|f_1+(\alpha_1-\beta_1)|^3$$

$$+ \tfrac{1}{2}|f_1-(\alpha_1-\beta_1)|^3\} \quad . \tag{D.16}$$

This normalized function is independent of frequency and velocity.

Equation D.16 then is the normalized clutter spectrum corresponding to one point on the ground. If ground position is varied along a line, a three-dimensional spectrum may be plotted to show spectrum change along the line. This is done in Figures 10 and 12 of Chapter V where it is shown that this function is approximately triangular shaped for typical airborne radar parameters.

VITA

Donald Carol Watson

Candidate for the Degree of

Doctor of Philosophy

Thesis: A STATE MODEL FOR AIRBORNE RADAR GROUND CLUTTER

Major Field: Electrical Engineering

Biographical:

Personal Data: Born in Fort Worth, Texas, December 30, 1930, the son of Una C. and Clayton C. Watson.

Education: Graduated from North Side High School, Fort Worth, Texas, in August, 1948; attended Arlington State College, Arlington, Texas, in 1954 and 1955; received the Bachelor of Science degree in Electrical Engineering from Texas A and M University in May, 1958; received the Master of Science degree in Electrical Engineering from Southern Methodist University in August, 1963; completed requirements for the Doctor of Philosophy degree in July, 1970.

Professional Experience: Radar systems engineer, General Dynamics Corporation, Fort Worth Division, 1958-1968.

Professional Organizations: Registered professional engineer in Texas; member of the Institute of Electrical and Electronic Engineers.